Characterization of Carbonaceous Aerosol

over the North Atlantic Ocean

by

Hansina Rae Hill

A Thesis Presented in Partial Fulfillment
of the Requirements for the Degree
Master of Science

Approved November 2010 by the
Graduate Supervisory Committee:

Pierre Herckes, Chair
Hilairy Hartnett
Paul Westerhoff

ARIZONA STATE UNIVERSITY

May 2011

ABSTRACT

Atmospheric particulate matter has a substantial impact on global climate due to its ability to absorb/scatter solar radiation and act as cloud condensation nuclei (CCN). Yet, little is known about marine aerosol, in particular, the carbonaceous fraction. In the present work, particulate matter was collected, using High Volume (HiVol) samplers, onto quartz fiber substrates during a series of research cruises on the Atlantic Ocean. Samples were collected on board the R/V Endeavor on West-East (March-April, 2006) and East-West (June-July, 2006) transects in the North Atlantic, as well as on the R/V Polarstern during a North-South (October-November, 2005) transect along the western coast of Europe and Africa.

The aerosol total carbon (TC) concentrations for the West-East (Narragansett, RI, USA to Nice, France) and East-West (Heraklion, Crete, Greece to Narragansett, RI, USA) transects were generally low over the open ocean (0.36±0.14 µg C/m^3) and increased as the ship approached coastal areas (2.18±1.37 µg C/m^3), due to increased terrestrial/anthropogenic aerosol inputs. The TC for the North-South transect samples decreased in the southern hemisphere with the exception of samples collected near the 15th parallel where calculations indicate the air mass back trajectories originated from the continent.

Seasonal variation in organic carbon (OC) was seen in the northern hemisphere open ocean samples with average values of 0.45 µg/m^3 and 0.26 µg/m^3 for spring and summer, respectively. These low summer time values are consistent with SeaWiFS satellite images that show decreasing chlorophyll a concentration (a proxy for phytoplankton biomass) in the summer. There is also a statistically significant ($p<0.05$) decline in surface water fluorescence in the summer. Moreover, examination of water-soluble organic carbon (WSOC) shows that the summer aerosol samples appear to have a higher fraction of the lower molecular weight material, indicating that the samples may be more oxidized (aged). The seasonal variation in aerosol content seen during the two 2006 cruises is evidence that a primary biological marine source is a significant contributor to the carbonaceous particulate in the marine atmosphere and is consistent with previous studies of clean marine air masses.

ACKNOWLEDGEMENTS

I am indebted to many individuals for their assistance during this thesis project; first and foremost, my research advisor, Dr. Pierre Herckes. His immense patience, relentless assurances, and tireless optimism regarding the project kept me on the path to completion.

It is important to note that, this project would never have got off the ground without the sample collection during the three cruises by Dr. Rainer Lohmann at the University of Rhode Island.

The assistance with instrumentation from a number of individuals at Arizona State University was critical for this project. My committee member Dr Paul Westerhoff allowed me to utilize both his Shimadzu total organic carbon analyzer (TOC-VCSH) and size exclusion chromatography with dissolved organic carbon detection (SEC-DOC) instrument. Chao-an Chiu and Jun Wang generously gave their time to run my samples on those instruments, respectively. Dr. Matt Fraser allowed me the use of his organic/elemental thermal optical transmittance analyzer and Andrea Clements' insight and willingness to troubleshoot throughout my analysis was indispensable. The Magnetic Resonance Research Center at Arizona State University, especially Dr. Brian Cherry, offered training and went above and beyond to help troubleshoot the low concentration issues of the samples on their Varian 500 MHz nuclear magnetic resonance instrument.

My committee member Dr Hilairy Hartnett deserves many thanks for her instruction in multiple courses, offer of expertise (especially related to marine chemistry), and exceptionally detailed feedback on my written work. I truly appreciate all the time she spent proofreading and offering suggestions. I could not have completed this thesis without her help.

Chlorophyll a satellite data was vital in analyzing seasonal data. Analyses and visualizations used in this study were produced with the Giovanni online data system, developed and maintained by the NASA GES DISC.

I would also like to gratefully acknowledge the NOAA Air Resources Laboratory (ARL) for the provision of the HYSPLIT transport and dispersion model and READY website (http://www.arl.noaa.gov/ready.php) used in this work.

TABLE OF CONTENTS

CHAPTER Page

LIST OF TABLES

LIST OF FIGURES

Figure Page

1. Introduction

The earth's atmosphere is made up gases, aqueous droplets, and particulate. The particulate in the atmosphere can range in size from a few nanometers to tens of microns and can be from natural sources such as dust, volcanic eruption, sea spray, or biomass burning; or from anthropogenic sources such as fuel combustion, industrial processes, or transportation.

Organic compounds comprise 20-90% of the aerosol particulate matter (Kroll and Seinfeld, 2008; Tyree, 2007) making this an important fraction of the total aerosol particulate. Historically, this has been an understudied portion of the atmospheric particulate. However, the variety in particle composition and the large uncertainties associated with the climactic effects by these particles (IPCC, 2007) has developed interest in the last decades (Gelencser, 2004).

Organic compounds are incorporated into atmospheric aerosol via two main pathways; the first being, the direct emission (natural or anthropogenic) from terrestrial and marine sources. The volatile organic compounds (VOC's) contained in these emissions can then be altered by oxidation to create new compounds (Kroll and Seinfeld, 2008; Pueschel, 1995; Rudich et al., 2007).

The organic compounds initially introduced into the atmosphere as aerosol particles are referred to as primary organic aerosol (POA), while the oxidized compounds formed in the atmosphere from gaseous precursors are considered secondary organic aerosol (SOA). The SOA, in turn, can be returned to the earth's surface by wet or dry deposition, oxidized to CO or CO_2, or oxidized to another organic aerosol and returned to the SOA pool. While this process allows removal of VOC's via photo-oxidation processes from the atmosphere, it adds a new and less characterized component to the already diverse atmospheric carbonaceous particulate. Also, the precise differentiation between POA and SOA becomes a little less clear in the case of combustion, where the SOA may form within seconds of being emitted (Gelencser, 2004) adding complexity to source determination.

1.1. Effects of Atmospheric Particulate Matter

Atmospheric particulate matter is ubiquitous in our environment and, as such, has some profound and easily observable impacts. Atmospheric carbonaceous particulate matter has been a societal issue well before the science was available to explain it. It's adverse effects on quality of life, visibility, health, and property has been documented as early as the 2nd century A.D. (Mamane, 1987).

One of the more obvious effects of particulate matter on our environment is visibility. Particulate accumulate in the atmosphere and scatters the light coming to our eyes. The result is diminished visibility. The brown haze, caused by nitrogen oxides, during smog events over large metropolitan areas is evidence of this.

Another well documented effect is that of health. Particulate can enter your lungs during respiration and then remain behind. A well know example would be black lung from prolonged exposure to coal dust. As early as the 13th century, following the importation of coal, ordinances were implemented in London to deal with the adverse health effects of this (Bowler and Brimblecombe, 1992). Later in the 17th century, Graunt (1662) suggests that the burning of coal may be responsible for the increased mortality rate in London over that of rural areas (Brimblecombe, 1978).

It wasn't until the 20th century, however, that the less immediate results of atmospheric particulate matter began to be investigated; it's effect on the earth's climate. With the interest in global climate change ever increasing, the influence of atmospheric particulate on the radiative balance of our planet is being examined in greater detail. Climate forcing, the occurrence of an altered planetary thermal equilibrium due to a change in the solar/thermal radiation (Lacis and Mishchenko, 1995), can occur directly or indirectly (Charlson and Heintzenberg, 1995).

The "direct effect" describes the absorption and scattering of incoming radiation by aerosols. Absorption by particulate can lead to atmospheric heating, while scattering, atmospheric cooling. This is affected by the optical properties of the aerosol. For instance, elemental carbon particulate, like soot, absorbs the incoming radiation, thereby warming the atmosphere.

The "indirect effect" relates to the ability of an aerosol to act as cloud condensation nuclei (CCN). Cloud droplets form on existing particles. These particles, or CCN, form dilute aqueous solutions and therefore generally reflect the incoming solar radiation (Finlayson-Pitts and Pitts, 2000). The more CCN available; the more droplets can form. The larger the number of droplets in the atmosphere, the smaller the droplet size (for a given volume of water), and the longer the lifetime of the cloud (Finlayson-Pitts and Pitts, 2000). This, in turn, leads to an increase in cloud albedo or reflectivity, which cools the atmosphere and creates a negative climate forcing effect.

1.2. Marine Atmospheric Particulate Matter

The concentration of carbon in marine atmospheric aerosols varies greatly depending on location (Figure 1). The source of the organic matter in the marine environment can be long-range transport of terrestrial

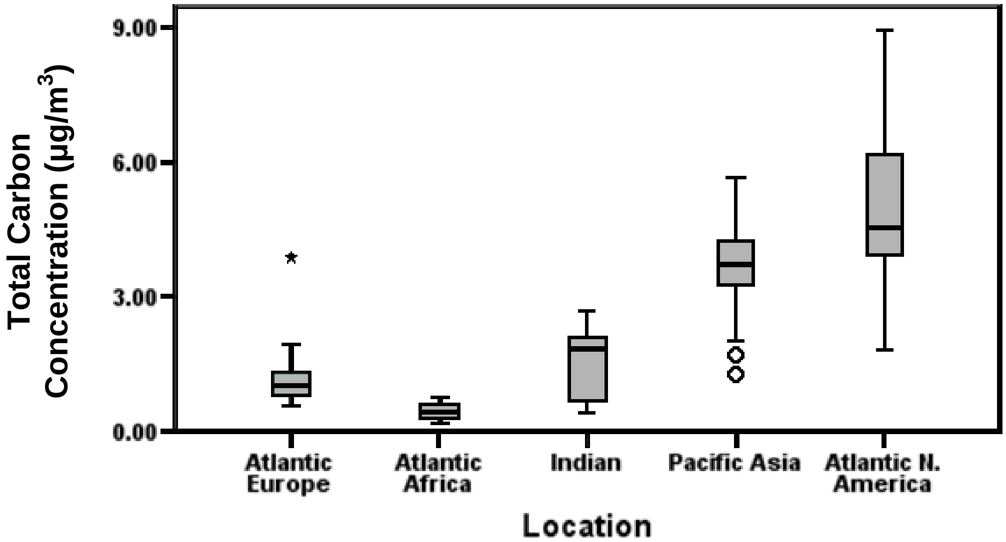

Figure 1. Histogram of the total carbon concentration for submicron marine samples (0.18-1.1μm) from 5 previous studies (Quinn and Bates, 2005).

carbon, ship emissions, sea spray, or secondary formation from marine precursors. The carbon concentration can be range from below detection limits, to values high enough to be compared with some urban areas (Tanner et al., 2004; Viana et al., 2007; Yttri et al., 2007; Yttri et al., 2009). The majority of this broad range can be explained by the sample collection location, since most of these measurements are made in close vicinity to the coast line in which the air mass back trajectories generally show recent terrestrial origin.

In an attempt to differentiate between marine atmospheric samples that contain large terrestrial inputs and those that are influenced mainly by the ocean (referred to herein as 'clean'), clean marine air masses have been defined to be those that have extremely low black or elemental carbon (EC) concentrations and air mass back trajectories that indicate at minimum of 2-3 days over the ocean. (Odowd et al., 1993) found that "clean" marine air masses had black carbon concentrations of ~20ng/m^3. Therefore, the concentration of carbonaceous atmospheric particulate in "clean" marine environments is considerably less than that of terrestrial areas with maximum total carbon values of ~1µgC/m^3 or less (Yoon et al., 2007). For samples collected in remote oceanic regions the ejection of carbon from sea into the atmosphere has been postulated to be an important carbon source (Carslaw et al., 2010).

Sea water can enter the atmosphere through direct ejection by crashing waves, wind shear, or the bursting of bubbles created by whitecap formation. The last is most likely the dominant mechanism (Buat-Menard, 1983). Bubble bursting ejects drops into the air in two distinct ways (Figure 2). First the thin surface of the bubble ruptures and sends small droplets into the air know as 'film drops'(Blanchard, 1963). The resulting hole in the ocean surface quickly fills by water running down the sides. At the bottom, the sea water running down the sides of the newly formed hole meet with enough force to expel drops into the air called 'jet drops' (Blanchard, 1963; Speil, 1999).

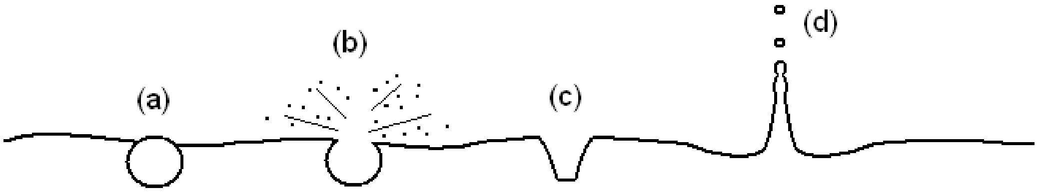

Figure 2. Surface bubble bursting mechanism; (a) single bubble at ocean surface, (b) formation of film drops, (c) filling of resulting hole, (d) formation of jet drops (Blanchard, 1963, 1982; Tyree, 2007).

The chemical content of these airborne drops is consistent with that of the upper marine layer, which is composed largely of salt, and to a lesser extent organic materials representative of the dissolved organic carbon (DOC) pool in the ocean. Recent studies that have examined the carbonaceous portion of air masses originating from marine environments [O'Dowd et al., 2004;Sciare et al., 2009] found a correlation between high phytoplankton abundance and an increase in atmospheric carbonaceous particulate concentrations.

Despite the importance of carbonaceous material in the environment, measurements from the marine systems are scarce compared to terrestrial sites, in particular urban sites. Still individual organic species, typically because of their toxicity, have received considerable attention (Gioia et al., 2008; Lohmann et al., 2009; Nizzetto et al., 2008; Zhang and Lohmann, 2010), but few studies focused on the bulk properties of the carbonaceous material.

The aim of the present study is to improve our understanding of the bulk properties of carbonaceous particulate in the marine boundary layer. This is achieved through the collection and subsequent analysis of total, organic, and elemental carbon concentrations in particulate matter collected aboard ship over the North Atlantic Ocean. Furthermore, the water solubility of the samples has been studied, as well as the oxygenation, saturation, and molecular size distributions of the water soluble fraction. The results are discussed with respect to the importance of biogenic contributions to marine particulate matter concentrations.

2. Instrumentation and Analyses

2.1. Sampling Locations

Atmospheric particulate matter samples were collected during three research cruises in the Atlantic Ocean (Figure 3); two in the North Atlantic and one spanning both the Northern and Southern hemispheres.

First, a series of samples was collected from October to November (2005) on board the *MS Polarstern* (Alfred Wegener Institute, Germany) during a North-to-South transect ranging over 74° (~ 8230 km), from 49°20’ N (Bremerhaven, Germany) to 24°50’S (Cape Town, South Africa).

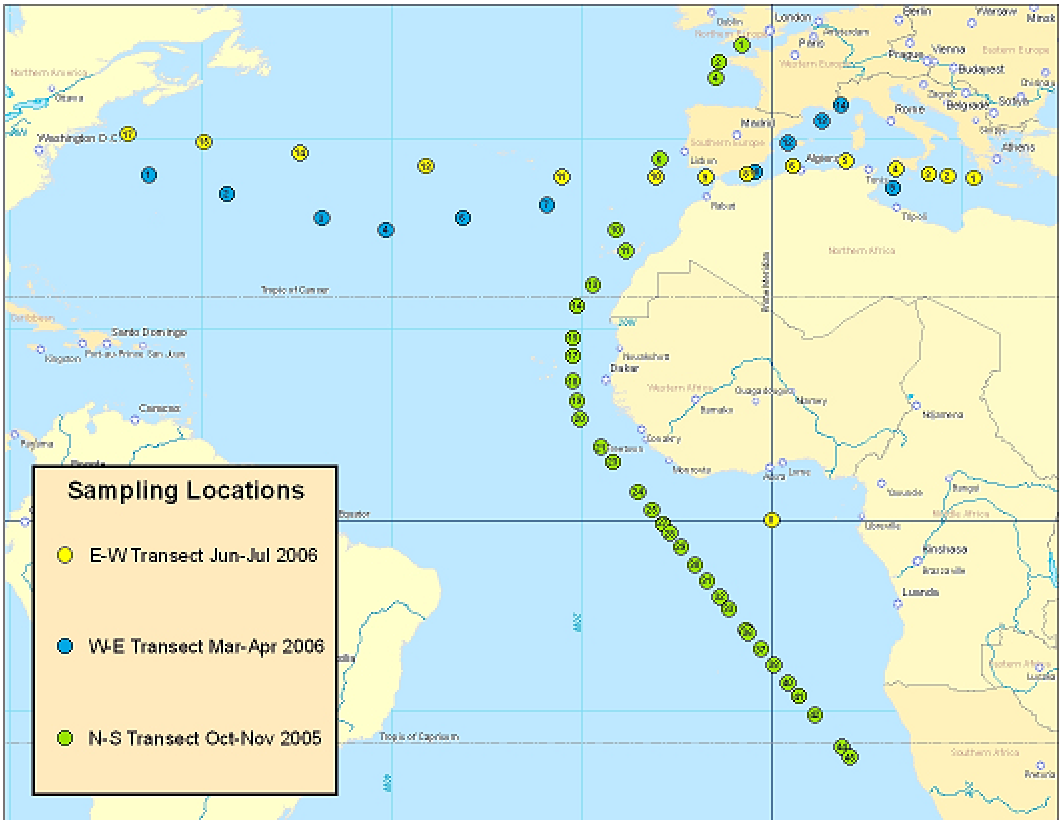

Figure 3. Sampling campaigns in the Atlantic Ocean.

Finally, samples in the North Atlantic Ocean were collected aboard the *R/V Endeavor* (University of Rhode Island, RI, USA) on a West-to-East transect (Narragansett, RI, USA to Nice, France) from March to April in 2006, and again in an East-to-West transect (Heraklion, Crete, Greece to Narragansett, RI, USA) from June to July 2006.

2.2. Aerosol Sampling

Total suspended particulate matter samples were collected using High Volume air samples (Tisch Environmental, Village of Cleves, OH, USA). The samplers were placed windward on the observation deck, 20 m above sea level, to minimize contamination from the ship (Nizzetto et al., 2008). Aerosol samples were collected on pre-combusted (600℃ for at least 8 hours) quartz fiber filters (Whatman, QM-A) Samples were stored frozen until analysis in the laboratory. In all cases, sampling duration varied between 24 and 48 hours.

2.3. Sampling Artifacts

Due to their strength, thermal stability, and low organic content, quartz fiber filters are commonly used for sampling atmospheric organic particulate (Gelencser, 2004). However, during particulate collection on quartz fiber filters, positive and negative artifacts may develop; either by adsorption of gaseous organics (positive) to the filter surface or by evaporation of volatile organics (negative) from the filter (Arp et al., 2007; Gelencser, 2004; Turpin et al., 1994).

2.3.1. Positive Artifacts

In order to account for positive artifacts, caused by adsorption of gas-phase molecules, a dual-filter system can be used. The assumption is that atmospheric particulate and gas-phase organics will collect on the front filter, while the back filter will only collect gas-phase species (Arp et al., 2007). Ideally, the adsorbed gas-phase organic molecules on the back filter indicate the magnitude of the positive artifact associated with the front filter (Subramanian et al., 2004). However, the back filter does not reach equilibrium immediately and sampling times less than 24 hours have been found to correspond to large variation in the positive artifact (Subramanian et al., 2004). Due to this effect and to low marine air particulate concentrations, the duration of sample collection lasted at least 24 hours.

While this system was only employed for one sample in the North-South transect, the organic carbon concentrations obtained through thermal optical transmittance, indicated that the back filter concentrations were those of the field blanks. For this reason, traditional field blank subtraction was deemed sufficient to account for any positive artifacts.

2.3.2. Negative Artifacts

Conversely, negative artifacts, that will cause underestimation of the total particulate concentration, involve desorption of semi-volatiles from the filter surface. While smaller in magnitude than adsorption artifacts (Turpin et al., 1994), this negative artifact can increase with changes in ambient conditions, such as temperature, or due to the initial removal of gas-phase organics via a denuder (Gelencser, 2004). With sampling durations of 24 hours or more, there is no way to avoid temperature fluctuations. Therefore, the sorption of the semi-volatile content of the sample will more closely resemble that of the temperature at the conclusion of sampling. For consistency, samples were removed at approximately the same time of day. To avoid the negative artifacts created by removal of the gas-phase organics, no denuder was employed.

2.4. Laboratory Methods

In order to evaluate the characteristics of atmospheric carbonaceous particulate over the Atlantic Ocean, several methods were employed: analysis of total, organic, and elemental carbon by thermal optical transmittance; detection of water soluble non-purgeable organic carbon through high temperature combustion with catalytic oxidation and non-dispersive infrared detection; determination of water soluble organic carbon size classes by size exclusion chromatography coupled to a UV/persulfate total organic carbon detector; and analysis of organic functional groups using proton nuclear magnetic resonance (NMR).

2.4.1. Organic, Elemental, and Total Carbon

Organic (OC), elemental (EC), and total (TC) carbon were determined using the thermal optical transmittance (TOT) method applied to a predetermined portion of the sample filter (Birch and Cary, 1996). The analysis was performed at Arizona State University in the laboratory of Professor Matt Fraser on a Laboratory OC EC Analyzer (Sunset Laboratories, Tigard, OR, USA).

The following is a detailed description of the process. In the first stage of this analysis, the quartz filter on which the aerosol is collected is placed in a helium atmosphere as the temperature is increased from ambient to 870ºC, thereby desorbing the organic carbon. The desorbed organic compounds are oxidized to CO_2 in the MnO_2 oven. The CO_2 is then converted to methane using a nickel catalyst and is detected using a flame ionization detector.

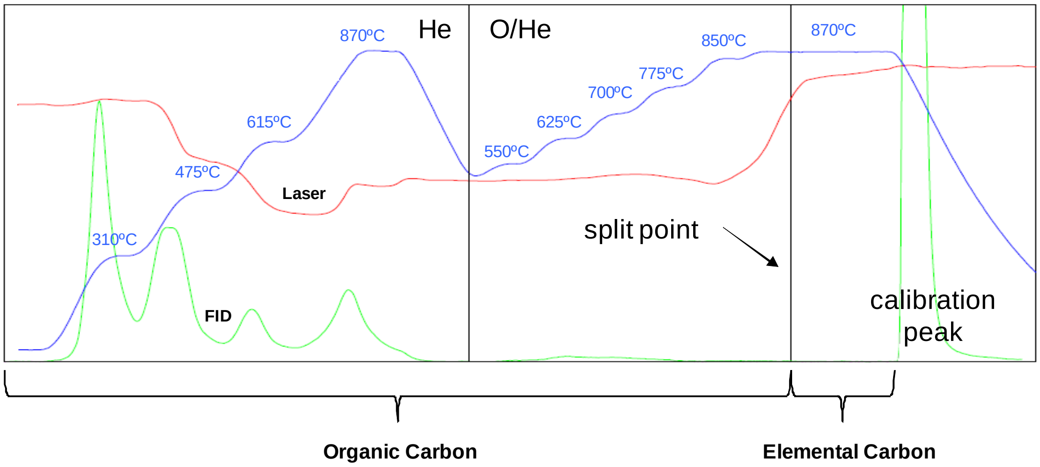

Figure 4. A representative thermogram acquired using the Sunset thermal optical transmittance (TOT) instrument. The blue line indicates the temperature profile; red, the laser reading; and green, the FID response. The split point indicates the cut-off for the organic carbon measurement and the start of elemental carbon measurement.

In the next stage, the temperature is reduced to 550ºC and the carrier gas is changed to Helium/Oxygen. The temperature is again increased; the elemental carbon is oxidized, converted to methane, and then detected. Throughout the entire process, a laser measures the transmittance from the filter. This transmittance can decrease during the first stage due to charring. Any charring would cause the EC measurement to be artificially higher. This is corrected for by determining the split point between the organic and elemental carbon; the point where the transmittance returns to its original value (Figure 4).

Some samples exhibit a double peak during the highest temperature block in the He-only atmosphere. This peak is generally attributed to carbonate carbon. The sample’s carbonate carbon concentration can be determined by difference through HCl fuming. This is done by placing the filter (1.0cm x 1.5cm) in a covered Petri dish surrounded by 8 to 12 drops of concentration hydrochloric acid for approximately 40 minutes. During the HCl fuming, the carbonate in the sample reacts with the HCl to produce carbon dioxide.

$$CO_3^{-2} + 2HCl \rightarrow H_2O + CO_2 + 2Cl^-$$

The sample is then analyzed as detailed above. The carbonate concentration is determined as the difference in organic carbon concentration between un-fumed and fumed portions of the filter.

Final OC, EC, and TC concentrations are reported in $\mu gC/m^3$ of air. Using the TOT data, µgC for the whole sample filter was determined, and then divided by the volume of air that passed through the collector.

$$OC_{\mu gC/m^3} = (OC_{\mu gC/cm^2} \text{ x } A_{\text{sample filter}})/V_{air}$$

The elemental and total carbon particulate concentrations were calculated similarly.

2.4.2. Water Soluble Organic Carbon and Total Dissolved Nitrogen

The water soluble portion of the organic carbon, as well as the total dissolved nitrogen, was determined using a Shimadzu total organic carbon (TOC-VCSH) analyzer with attached total nitrogen unit (TNM-1). The analysis was performed at Arizona State University in the laboratory of Dr. Paul Westerhoff.

For this determination, filter fractions were extracted in high purity water (Millipore System, MA, USA; >18MΩ/cm), filtered, and then the dissolved organic carbon in the extract was determined. In detail, a portion of the sample filter was added to a screw cap vial along with 10mL of Milli-Q™ water and sonicated for 30 minutes. The aqueous extract was decanted and set aside. This process was repeated once and the total extract was filtered through a pre-fired (450ºC overnight) glass microfiber filter (Whatman, GF/F). The filtered extract was acidified with hydrochloric acid to convert the inorganic carbon (IC: carbonate, bicarbonate) into carbon dioxide.

During analysis, the CO_2 that resulted from the IC, was removed by sparging with a CO_2 free gas. Since volatile organic carbon (VOC) can be lost during this process, the carbon detected during this analysis is considered non-purgeble organic carbon, however, for the case of simplicity, it will be referred to as water-soluble organic carbon (WSOC) throughout this text. The IC-free extract was then injected (75 µL) into a heated combustion tube (720ºC) where an oxidation catalyst (platinum on alumina) converted the remaining carbon to CO_2. Concurrently, the nitrogen compounds and ammonium were oxidized to NO, while the NO_2^-

and NO_3^- were reduced to NO (Pan et al., 2005). The CO_2 was detected by a non-dispersive infrared gas analyzer (NDIR) and the NO by a chemiluminescence detector.

Each sample injection was repeated 3 to 5 times per sample automatically. If the standard deviation of the first 3 injections was greater than 0.1mg/L, the sample was run and 4th and sometimes a 5th time.

Final WSOC and total dissolved nitrogen (TDN) concentrations are reported in µgC/m^3 of air. Using the WSOC and TDN data, the mass of carbon or nitrogen on the whole sample filter was determined and then divided by the volume of air that passed through the collector.

$$\mathrm{WSOC}_{\mu gC/m^3} =$$

$$[(\mathrm{WSOC}_{\mu gC/mL} \times V_{\text{used in extraction}})/(A_{\text{filter used in extraction}})] \times (A_{\text{sample filter}}/V_{\text{air}})$$

The total dissolved nitrogen in air concentrations were determined similarly.

2.4.3. Water Soluble Organic Carbon Size Fraction

Molecular size separation of dissolved organic carbon (DOC) can be obtained using a variety of techniques; size exclusion chromatography (SEC), ultrafiltration (UF), and field flow fractionation (FFF) are the most prominent (Shon et al., 2006).

Size exclusion chromatography works on the principle that molecular diffusion into the pores of a stationary phase differs depending on the size of the molecule. In principle, larger molecules are less likely diffuse into the small pores so they move through the column more quickly than smaller molecules which are retained longer. When calibrated with a standard, the molecular size can be related to retention time. The small sample volume required makes SEC ideal for atmospheric DOC analysis as compared with UF and FFF. Recently, SEC has been used to fractionate the WSOC of aerosols (Andracchio et al., 2002; Samburova et al., 2005) and fogs (Krivacsy et al., 2000).

Detection of solutes after size separation has been performed primarily by UV absorption at 254 nm, because of the strong absorption of organic matter at this wavelength. UV radiation, however, specifically affects conjugated pi systems and therefore will only detect those organic molecules containing a double bond. In order to detect saturated organic constituents such as alkanes, the DOC eluent can be oxidized to CO_2 and detected by Fourier transform infrared spectroscopy (FTIR) or mass spectrometry (Warton et al., 2008). Alternatively, an online DOC analyzer utilizing a conductivity detector can be used (Her et al., 2002a; Her et al., 2002b; Nam and Amy, 2008). The data presented here was collected using SEC-DOC with UV/persulfate oxidation to CO_2 and subsequent detection by conductivity.

Samples were first extracted into Milli-Q™ water using a method similar to that for WSOC detection. Size exclusion chromatography was performed using high performance liquid chromatography (WATERS 2695 Separation Module) followed by dissolved organic carbon detection (modified Sievers Total Organic Carbon Analyzer 800 Turbo). A TSK 50S column (TOSOH TOYOPEARL HW-50S resin) was used for SEC with a phosphate buffer mobile phase (0.0024M NaH_2PO_4 and 0.0016M Na_2HPO_4, pH=6.8, 0.025M Na_2SO_4, ionic strength = 0.1M, conductivity = 4.57mS). Samples were adjusted, using concentrated eluent (40x), for conductivity prior to analysis.

Samples were injected (1mL) at a flow rate of 1mL/min and DOC data was collected every 0.5 seconds (WATERS Empower, Milford, MA, USA). Size calibration was achieved with polyethylene glycol standards (PEG; Sigma Aldrich, 10mg/L; 200, 600, 1000, 1450, 3350, 4600, 8000, 10000 Da). A blank of Milli-Q™ water was examined for each samples set.

The DOC response (recorded every 0.5 seconds) lead to 12,000 data points for over 100 minutes of run time. To reduce this number, the

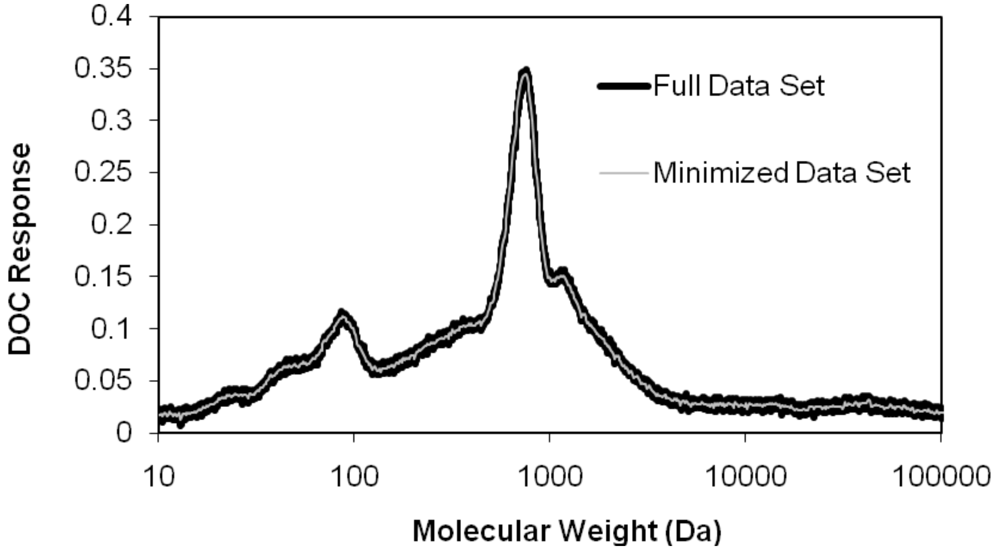

Figure 5: Comparison between the full data set (12,000 data points) and the minimized data set (1,000 data points) used for SEC-DOC analysis.

data was averaged every 12 points, creating 1000 data points in the final data set. The effect of the data reduction was negligible (Figure 5) as shown by the peak shape and DOC response retained in the reduced data set. After data reduction, the baseline was manually corrected.

2.4.4. Proton Nuclear Magnetic Resonance

The complexity of atmospheric aerosols makes characterization at a molecular level impossible. Instead, recent efforts have focused on methods that can characterize the functional groups present in aerosol material including FTIR (Maria et al., 2002; Schwartz et al., 2010) and ^{1}H-NMR (Cavalli et al., 2004; Decesari et al., 2007). The latter was applied in the present study due to its suitability for small volume aqueous samples.

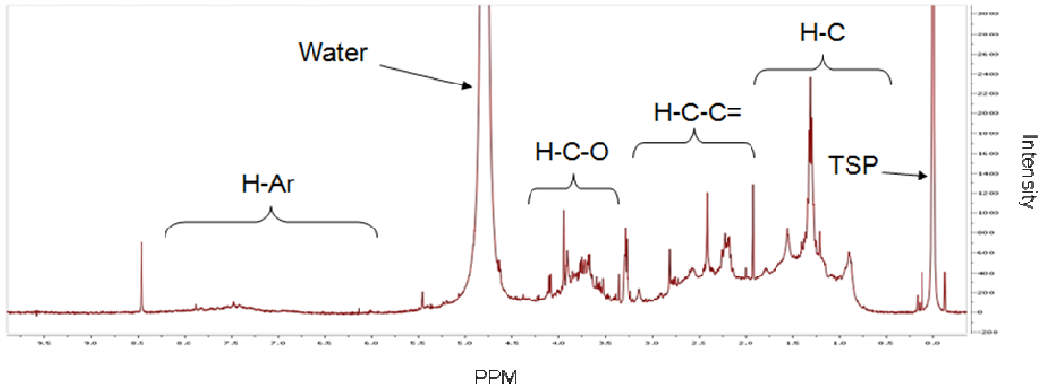

Figure 6. A representative proton NMR spectra showing the integration regions used during the analysis.

A portion of the filter, 4.91cm^2, was cut up using a razor blade and added to a pre-cleaned screw cap vial along with 1mL of a deuterium oxide solution containing 0.00375 wt% 3-(trimethylsilyl)propionic-*2,2,3,3-d*$_4$ acid, sodium salt (Sigma Aldrich, 99.9 atom % D, contains 0.05 wt. % 3-(trimethylsilyl)propionic-*2,2,3,3-d*$_4$ acid, sodium salt (TSP)). The vial was capped and sonicated for 30 minutes. The resulting extract was filtered through a glass fiber filter (Whatman, GF/F grade). The final solution was then placed in a quartz 500MHz NMR tube and run overnight on the Varian 500MHz NMR in the Magnetic Resonance Research Center at Arizona State University.

Spectra were phase and baseline corrected using MestreNova 5.2 analysis software (Mestrelab Research, Escondido, CA, USA). All spectra were referenced to TSP. To determine the total proton concentration extracted by the solvent, the entire spectra (12 to -1ppm) was integrated and the water peak subtracted. The final integration value was compared to the integration of the reference peak to get total proton content.

Integration of specific regions of the spectra were performed using chemical shifts laid out by (Decesari et al., 2007): 0.5-2.0 ppm [H-C], 2.0-3.4 ppm [H-C-C=], 3.5-4.1 ppm [H-C-O], 6.5- 8.4 [H-Aromatic] (Figure 6). The integration values were normalized to the unsaturated aliphatic [H-C] region for that particular spectrum.

2.4.5. Chlorophyll a and Fluorescence

Chlorophyll a concentrations data was acquired from NASA's satellite SeaWiFs. Analyses and visualizations used in this study were produced with the Giovanni online data system, developed and maintained by the NASA GES DISC. The data presented is a monthly average during both the spring and summer sampling times

Continuous fluorescence measurements for chlorophyll a were taken of the surface ocean water using Turner Designs 10-AU-005 continuous flow fluorometer. Fluorescence measurements were then averaged over the open ocean for the duration of each atmospheric sample collected.

2.5. Quality Assurance and Control

2.5.1. Sampling and Sample Storage

Before collection the quartz fiber filters were covered in aluminum foil and baked at 600ºC overnight. After collection, samples were returned to their aluminum foil envelopes, placed in a Ziploc storage bag, and stored in the freezer (-20℃) until analysis.

2.5.2. Glassware Cleaning

All glassware was cleaned to remove residual organic compounds before use. The cleaning process consisted of cleaning with a detergent (Alconox), followed by rinsing twice each with tap water, DI water, and finally ultrapure (Milli-Q™) water. The glassware was allowed to air dry and then rinsed with 2-propanol (Optima Grade). After the 2-propanol evaporated, the glassware was covered with aluminum foil and heated in a furnace for no less than 8 hours at 450ºC.

2.6. Laboratory Analysis Uncertainties and Detection Limits

For all OC, EC and TC analyses, ten percent of all sample sets were run in triplicate and the uncertainty is reported as the resulting average relative standard deviation of the triplicates and applied to all samples. Duplicate filter portions were run every 10 samples to check for reproducibility. Limit of detection was determined to be 3 times the standard deviation of the field blanks (15 ng/m^3). Instrument accuracy was checked daily using a sucrose standard.

To determine the uncertainty for WSOC and TDN analyses, each sample was injected in triplicate to determine a standard deviation. The extraction was duplicated every ten samples (when enough filter was present) to examine the reproducibility and the reported uncertainty is the average relative standard deviation of these duplicates. The instrument was calibrated daily with potassium hydrogen phthalate.

Table 1
List of integration regions used when determining uncertainty for ^{1}H-NMR.

	Decesari et al., 2007 (ppm)	Bruice, 2001 (ppm)	Reich, 2008 (ppm)
H-C	0.5 - 2.0	0.8 - 1.6	0.7 - 1.8
H-C-C=	2.0 - 3.4	1.7 - 3.2	1.8 - 3.4
H-C-O	3.5 - 4.1	3.2 - 4.3	3.5 - 4.3
H-Ar	6.5 - 8.4	6.5 - 8.0	6.3 - 8.2

Because both electronegativity and the attached substituents affect the proton chemical shift, the ranges used by Decesari et al. (2007) cannot be exact. To test the viability of these integration regions, slight modifications were made to the ranges, based on published data (Bruice, 2001; Reich, 2011), in order to examine what effect small alterations might have on the results (Table 1). The data was process using the above chemical shift regions from which an average and standard deviation was determined. The uncertainty was determined to as one standard deviation.

3. Results

In order to examine samples over a broad area, they were first analyzed individually, but then grouped according to transect (E-W transects versus N-S transect), season (Spring versus Summer), and finally, location within the transect (Open Ocean versus Coastal Ocean).

3.1. Coastal versus Open Ocean

Two distinct categories of marine samples were defined based on the samples' concentration of elemental carbon. Open ocean samples, were defined as those samples with the least amount of terrestrial input. Since elemental carbon (EC) is a product of combustion, samples with the lowest levels of EC have the least amount combustion inputs. With the exception of combustion aboard marine vessels, which only comprises 3.5% (Buhaug et al., 2009) of the global carbon emissions, the majority of combustion occurs in terrestrial environments. Therefore, the lowest concentrations of EC would indicate the least amount of terrestrial input. This was shown in carbonaceous aerosols measurements from Mace Head, Ireland (O'Dowd et al., 1993) where the "cleanest" Atlantic Ocean air masses spent 2-3 days over the open ocean and contained an average of 13ng/m^3 EC. Equivalent black carbon concentrations from air masses over the Austral Ocean collected at Amsterdam Island averaged 5.8ngC/m^3 (Sciare et al., 2009). Considering the previous findings for marine air mass particulate EC concentrations and the TOT limit of detection (15ngC/m^3), samples defined herein as "open ocean" are those with an EC concentration at or below the detection limit.

3.2. Organic/Elemental/Total Carbon

3.2.1. The East-West Transects

The average OC/EC concentrations for the E-W transects in spring and summer were 1.18/0.16 µg/m^3 and 1.63/0.27 µg/m^3, respectively. Total carbon concentrations of the marine aerosols are determined by the addition of OC concentration with the EC concentration, giving 1.34 µg/m^3 and 1.90 µg/m^3, for spring and summer, respectively. Both data sets showed increased OC and EC concentrations as the ship entered the coastal areas (approximately -70º to -60º longitude and -5º to 25º

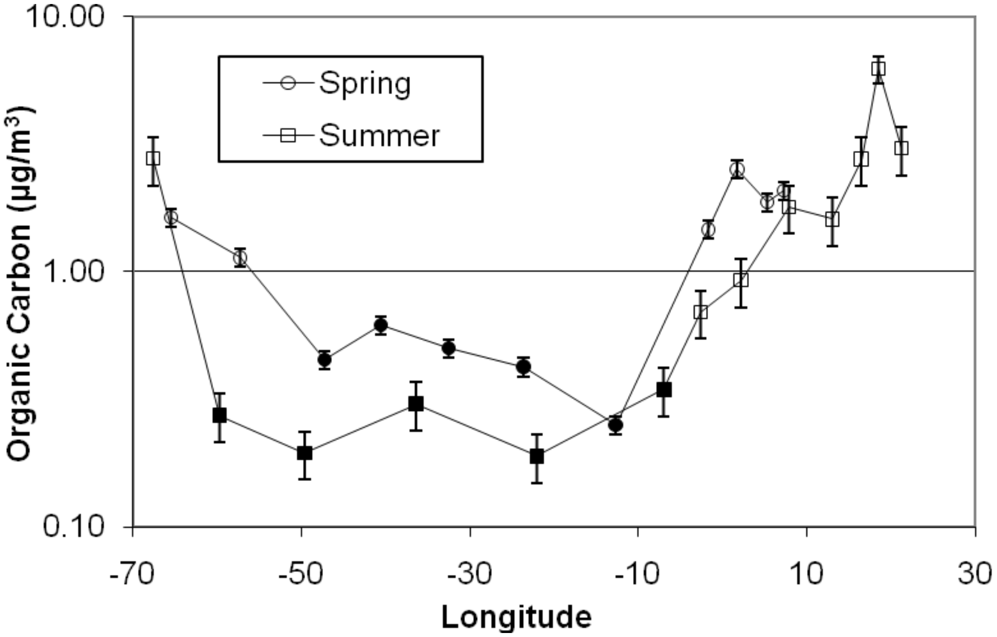

Figure 7. Organic aerosol carbon concentrations determined by TOT for spring (circle) and summer (square) North Atlantic cruises. Unfilled shapes indicate coastal ocean samples and filled shapes indicate open ocean samples. Error bars indicate the average relative standard deviation of 10% of the samples.

longitude). The greatest carbon concentrations were found in samples collected from the Mediterranean Sea with lower coastal carbon concentrations in samples collected off the NE coast of the of the United States. Organic carbon concentrations for the spring (March-April) and summer (June-July) 2006 cruises are shown in Figure 7. The spring cruise samples are denoted with circles and summer cruise samples, squares. Filled markers indicate samples that fit the definition of open ocean (Section 3.1). The average OC for open ocean samples is 0.45 and 0.26 µg/m^3 for spring and summer, respectively. The difference between these values was found to be statistically significant ($p<0.05$).

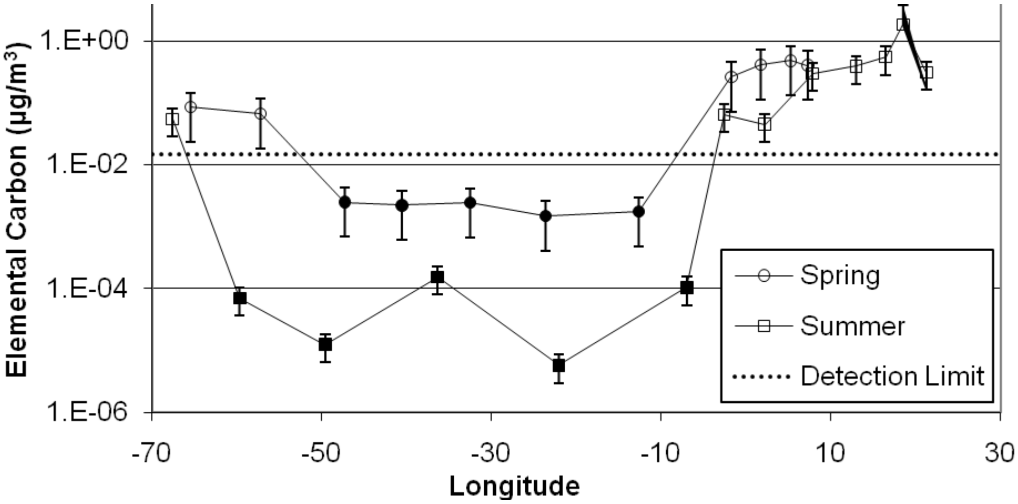

Figure 8. Elemental aerosol carbon concentrations determined by TOT for spring (circle) and summer (square) North Atlantic cruises. Five samples in both the spring and summer fell below the detection limit, defining them as open ocean samples. Error bars indicate the average relative standard deviation of 10% of the samples.

Similarly, Figure 8 shows the EC concentrations for the E-W transects. Five samples in both the spring and summer fell below the detection limit (not shown), defining them as open ocean locations. As with the OC concentrations, EC was found to be of higher concentration in samples collected in the Mediteranean Sea, than of the Northeast Coast of the United States; as much as 4 times higher.

3.2.2. The North-South Transect

The OC and EC concentrations, as well as the 72 hour air mass back-trajectory, for the North-South transect are shown in Figure 9. The highest OC and EC concentrations are found in samples off the coast of Europe with back-trajectories that originate over land, similar to findings from the East-West spring and summer cruises. The OC and EC concentrations decreased substantially in the southern direction with the exception of a small increase near the 15° north latitude. The air mass back-trajectories for these samples show a terrestrial origin, indicating that the increase in atmospheric particulate carbon for this area may be from anthropogenic or

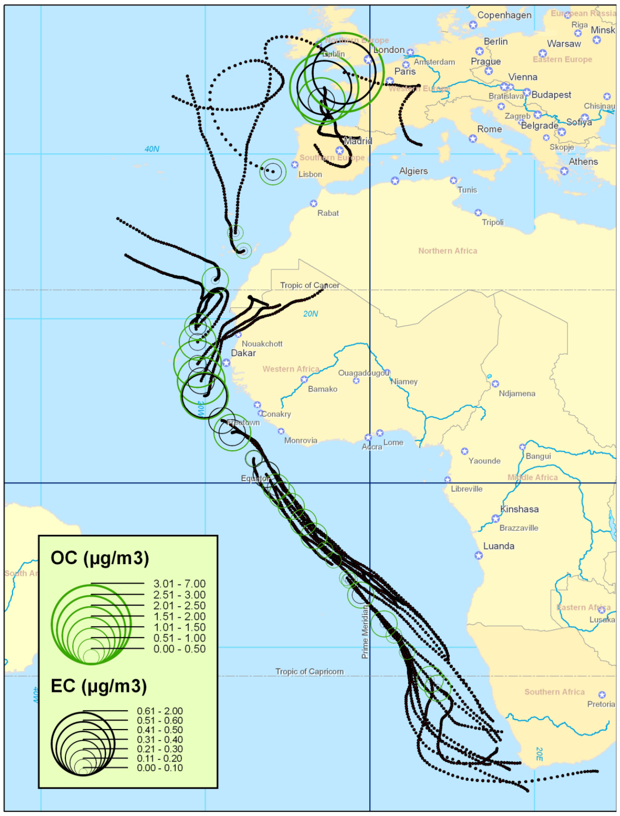

Figure 9. Atmospheric particulate organic carbon (green) and elemental carbon (black) concentrations and 72hr air mass back-trajectories.

terrestrial biogenic inputs. In addition, previous work in this area found an increase in Levoglucosan (Pierre Herckes, personal communication, April 14, 2011) a molecular marker for biomass burning, indicating the OC and EC increases may be due, in part, to biogenic combustion.

3.3. Water-Soluble Organic Carbon and Total Nitrogen

3.3.1. The East-West Transects

3.3.1.1. Water-Soluble Organic Carbon

Water-soluble organic carbon (WSOC) was measured in samples from both the spring and summer cruises. Similarly to OC, the concentration of WSOC (Figure 10) was found to be higher near the coastal areas than in the open ocean, with the highest coastal area

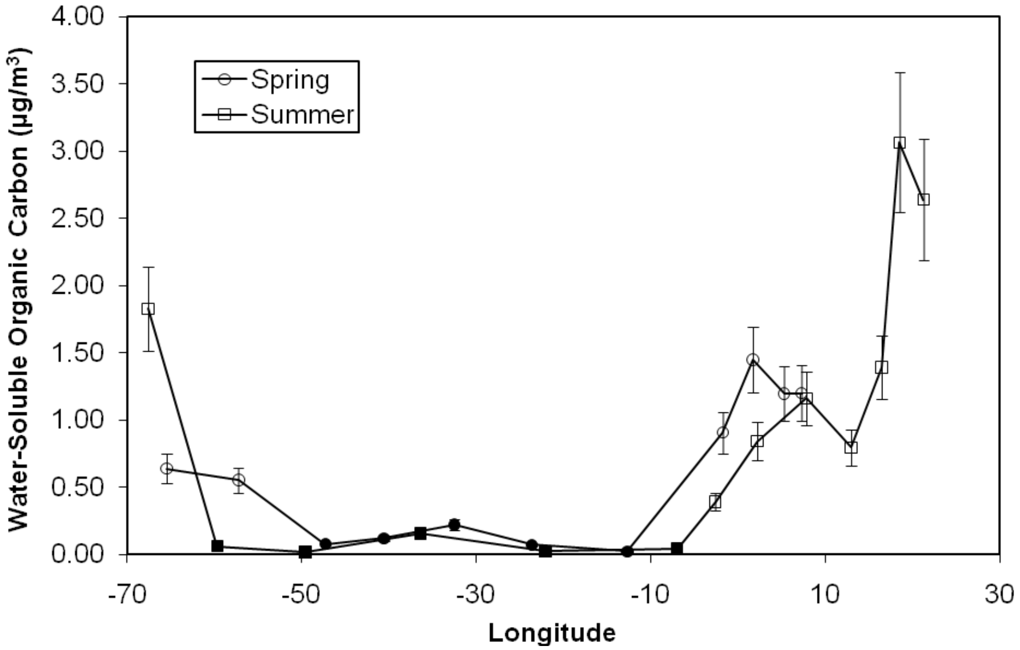

Figure 10. Water-soluble organic carbon concentrations determined for spring (circle) and summer (square) North Atlantic cruises. Unfilled shapes indicate coastal ocean samples and filled shapes indicate open ocean samples.

concentrations found in samples from the Mediterranean Sea. Unlike the OC concentrations, however, the average WSOC for spring and summer are not significantly different with 0.10±0.07 $\mu g/m^3$ and 0.06±0.06 $\mu g/m^3$, respectively. This lack of a seasonal pattern is consistent with data on WSOC from the Austral Ocean atmosphere (Sciare et al., 2009).

Because the overall OC changes significantly between samples, especially in the open ocean, it is common to examine the %WSOC.

$$\text{WSOC } (\mu g/m^3) \,/\, \text{OC } (\mu g/m^3) * 100 = \text{\%WSOC}$$

Analysis of the %WSOC, instead of the total concentration of WSOC, will show the possible change in the water-solubility of the organic carbon present, which can provide insight into the age of the particulate. For instance, the higher the %WSOC may indicate more "aged" or oxidized

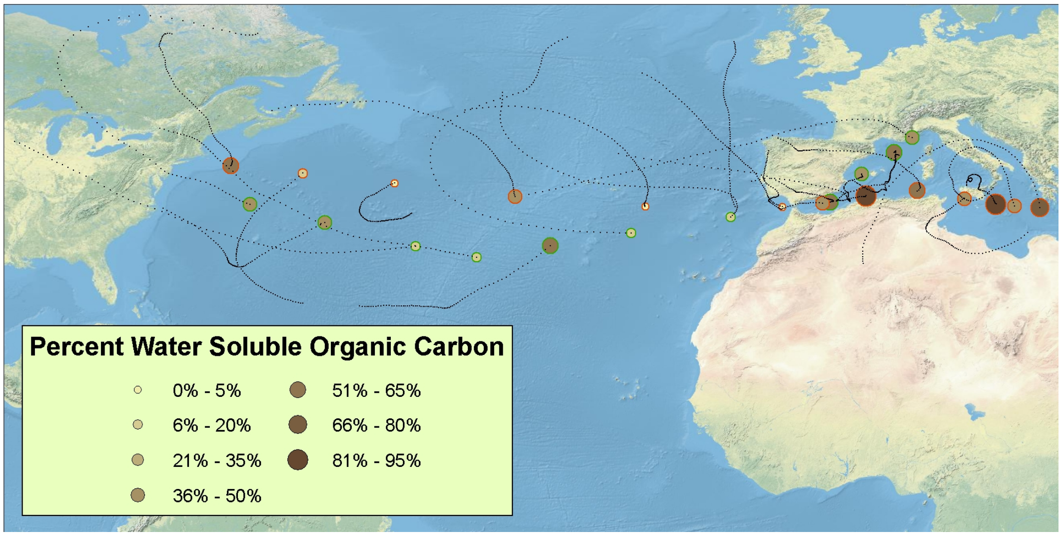

Figure 11. Percent water-soluble organic carbon concentrations expressed as a percentage of total particulate OC for the spring (green) and summer (red) cruises. Dotted lines indicate the 72 hour back-trajectory.

particulate (Kondo et al., 2007; Miyazaki et al., 2006).

Analysis of the %WSOC atmospheric concentration shows a higher percent in the coastal areas with the exception near -30° longitude (Figure 11). The cause for the unexpected increase in this location is not yet clear, since these particular samples do not share a common air mass back-trajectory or show any discernable differences in the chlorophyll a concentrations or the marine surface water fluorescence (Section 4.6).

Alternatively, the water-insoluble organic carbon (WIOC) portion can be analyzed by taking the difference between the OC and WSOC. It has been stated that the WIOC portion of the atmospheric particulate should be less oxidized in nature and therefore be considered a primary emission (Sciare et al., 2009). If this is the case, then increased WIOC would be seen during times of increased biogenic activity in the open ocean samples. The WIOC concentration of the open ocean samples collected during the 2006 cruises were averaged for the spring and summer open ocean samples. There is a significant difference ($p<0.05$) between the spring (0.35 $\mu g/m^3$) and summer (0.20 $\mu g/m^3$) WIOC average concentrations. Previous studies in the North Atlantic show agreement with this (Cavalli et al., 2004; O'Dowd et al., 2004; Yoon et al., 2007).

3.3.1.2. Total Dissolved Nitrogen

The total dissolved nitrogen was determined for the E-W transect samples only. The TDN, like the total carbon particulate concentration, was higher in the coastal areas (Figure 12), with the Mediterranean Sea samples being the highest overall. Unlike the OC concentrations however, the spring and summer open ocean samples showed no statistically significant difference, with an average of 0.15±0.06 µg/m^3 and 0.12±0.05 µg/m^3, respectively.

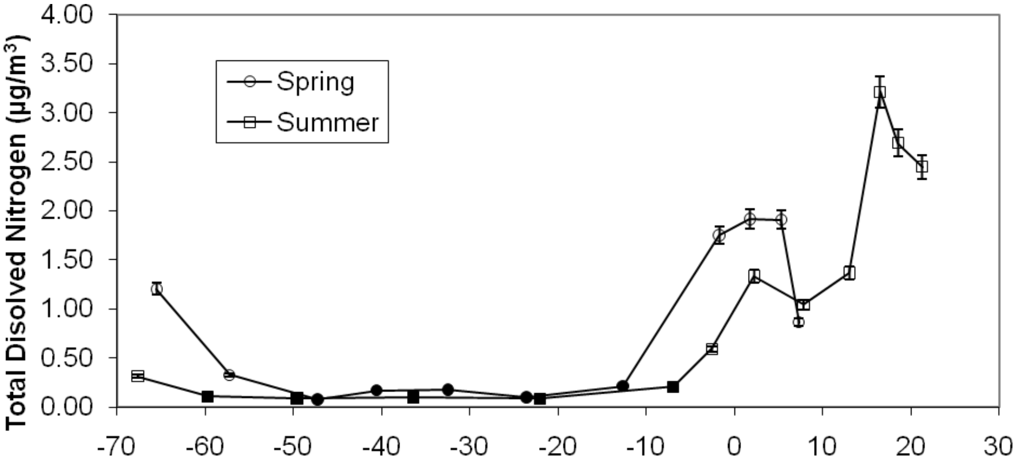

Figure 12. Total dissolved nitrogen concentration determined in the water-soluble fraction of the particulate for the spring (circles) and summer (squares) cruises. Filled shapes indicate open ocean samples and unfilled shapes indicate samples obtained in coastal areas.

3.4. Size Exclusion Chromatography

3.4.1. The East-West Transects

Since the size of the atmospheric particulate may relate to the amount of oxidation that has occurred (higher molecular weight indicating less oxidation of the particulate), the water-soluble organic carbon portion of the atmospheric particulate was examined using size exclusion chromatography (SEC). Due to availability, only the samples collected during the East-West transects were examined of the three cruises.

A representative example of a coastal and open ocean chromatogram is shown in Figure 13. The shapes of both chromatograms are similar in that they have a broad peak between 20,000 and 65,000 Da and two narrower peaks, one from 800 to 900 Da and the other from 400 to 500 Da, with the largest peak being between 800 and 900 Da. The difference lies in the lower molecular weight peaks. The open ocean sample has a local maximum at approximately 100 Da, whereas the coastal ocean sample local maximum occurs at approximately 30 Da. It should be noted, however, that this area falls below the lowest molecular

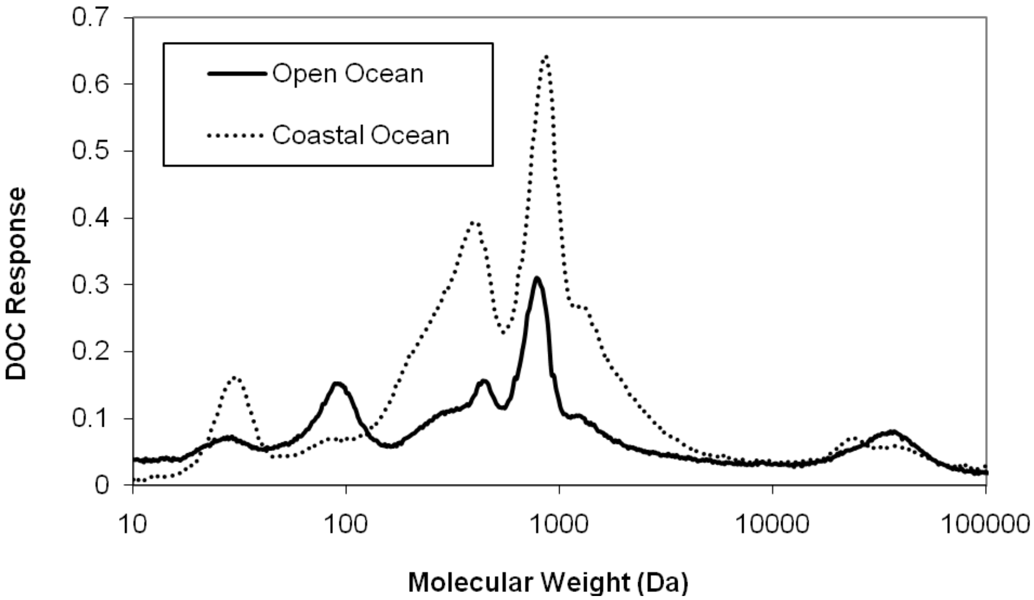

Figure 13. A representative plot of molecular weight versus DOC response for an open ocean (solid line) and a coastal ocean (dotted line) sample.

weight (MW) sample (200 Da) in the calibration curve, so the exact MW cannot be determined with any certainty.

A second area of comparison is between the spring and summer open ocean samples. Representative peaks are shown in Figure 14. The largest peak in both spring and summer samples is, as above, between 800 and 900 Da. There is also a notable shift in the chromatogram to lower MW's in the summer sample compared to the spring sample. This shift becomes more noticeable as the MW decreases. However, as noted above, the exact MW below 200 Da is uncertain, since this is below the PEG calibration curve. Still, this shows a larger fraction of the WSOC coming from smaller molecules in the summer. The summer sample also has a larger peak at a very high MW (~40,000Da), which is minimal in the

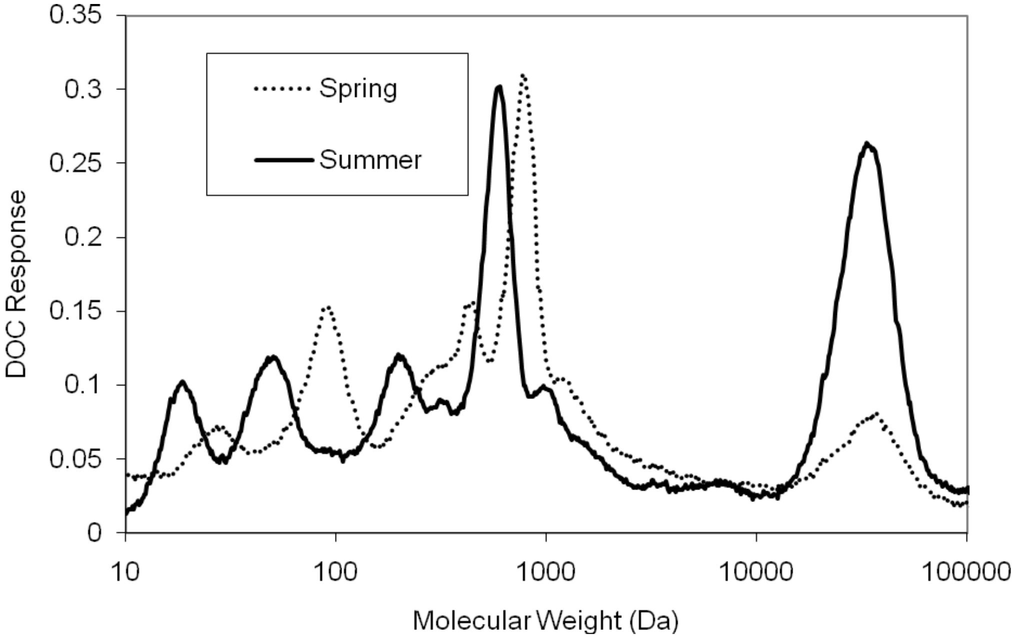

Figure 14. A representative plot of molecular weight versus DOC response for a spring (dotted line) and a summer (solid line) open ocean sample.

spring sample.

3.5. Molecular Oxygenation and Saturation

The bulk proton NMR characteristics were examined by integrating over four regions of the spectrum corresponding to specific functional groups (See section 2.4.4). The region of the spectrum corresponding to aromatic compounds in most cases could not be distinguished above background and was therefore not considered. Also, not all samples were examined for their functional group content using proton NMR. For this reason, the samples that were studied from the East-West transects and the North-South transect were grouped together according to coastal or open ocean properties.

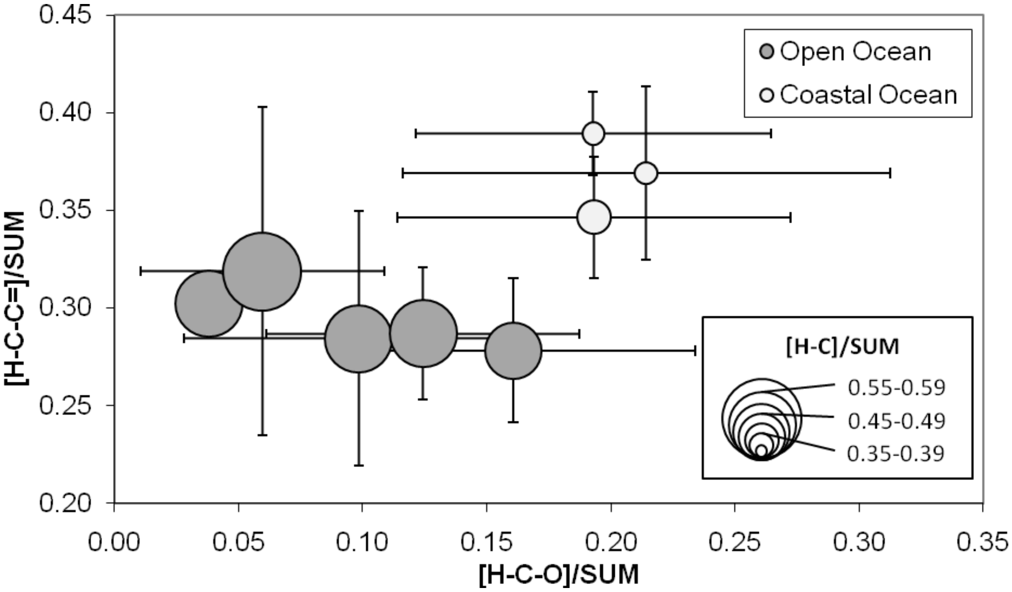

Figure 15. Index of oxygenation versus saturation of open ocean and coastal ocean samples. All values are the ratio of the integrated area corresponding to the particular functional group (oxygenated aliphatic [H-C-O], unsaturated aliphatics [H-C=C], or saturated aliphatics [H-C]) to the sum of all integrated areas.

A comparison of the functional group content for coastal and open ocean samples is shown in Figure 15. Oxygenated aliphatic [H-C-O] were plotted against unsaturated carbons connected to a saturated one [H-C=C]. The size of the circle indicates the saturated aliphatic [H-C] portion. All values are a ratio of the integrated area corresponding to the particular functional group and the sum of all integrated areas.

Marine samples considered open ocean, appear to have a higher ratio of saturated aliphatic compounds and a lower ratio of oxygenated groups, while the coastal areas have a smaller ratio of saturated aliphatic compounds, but a larger ratio of the oxygenated groups.

3.6. Fluorescence in the Open Ocean

Continuous fluorescence measurements for chlorophyll a were taken of the surface ocean water for the spring and summer sampling events. Fluorescence is directly proportional to the concentration of Chlorophyll a, so an increase in fluorescence may indicate an increase in phytoplankton population. Fluorescence measurements were averaged over the open ocean (Figure

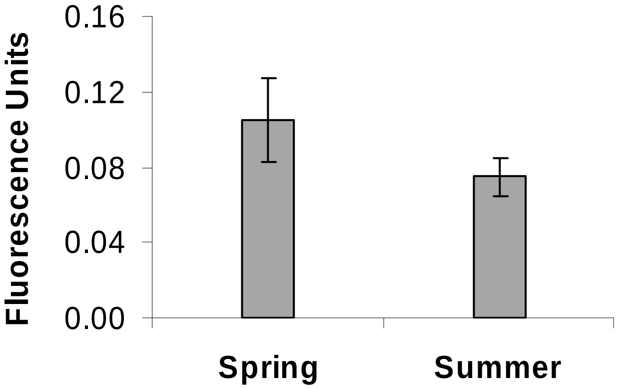

Figure 16. Average surface ocean fluorescence data for the spring and summer North Atlantic cruises. The bars indicate ± 1 STD.

16). A t-test indicates that these two averages are statistically significant ($p < 0.05$).

4. Discussion

Characterization of atmospheric marine particulate has been largely unexamined. This is especially true for the carbonaceous portion, which has only recently gained interest. Since sample collection was aboard ship instead of land based, these samples offered a rare opportunity to gain further insight into this area.

There were two prevailing questions throughout this project. First, are there significant differences in the carbonaceous component of the atmospheric marine particulate matter in different locations and if so what are they? And second, are there significant differences in the carbonaceous atmospheric marine particulate matter collected in different seasons and if so what are they? To answer these questions, samples were categorized as either coastal or open ocean locations and as either the spring or summer season.

4.1. Coastal versus Open Ocean Atmospheric Particulate

4.1.1. Organic and Elemental Carbon

As previously mentioned, TOT was used to determine the OC and EC. Organic carbon can form through gas phase oxidation or come from a primary source. It can directly affect the global climate by either scattering or absorbing light. Elemental carbon, which is a product of combustion, directly effects the global climate by absorbing light thereby heating the atmosphere.

Analysis of the particulate matter samples from the marine environment showed a clear difference in the concentrations of OC and EC between the coastal and open ocean, with higher and lower concentrations, respectively; supporting the use of the EC concentration to differentiate between the coastal and open ocean samples. The coastal ocean had higher concentrations of both carbonaceous particulate subsets. Terrestrial, natural and anthropogenic, inputs were undoubtedly the cause of this, since samples where air masses spent time over land, i.e., samples collected in the Mediterranean Sea and off the Northeast coast of the United States (Figure 17) or samples collected off the coast of Africa (Figure 9), showed increases in both OC and EC.

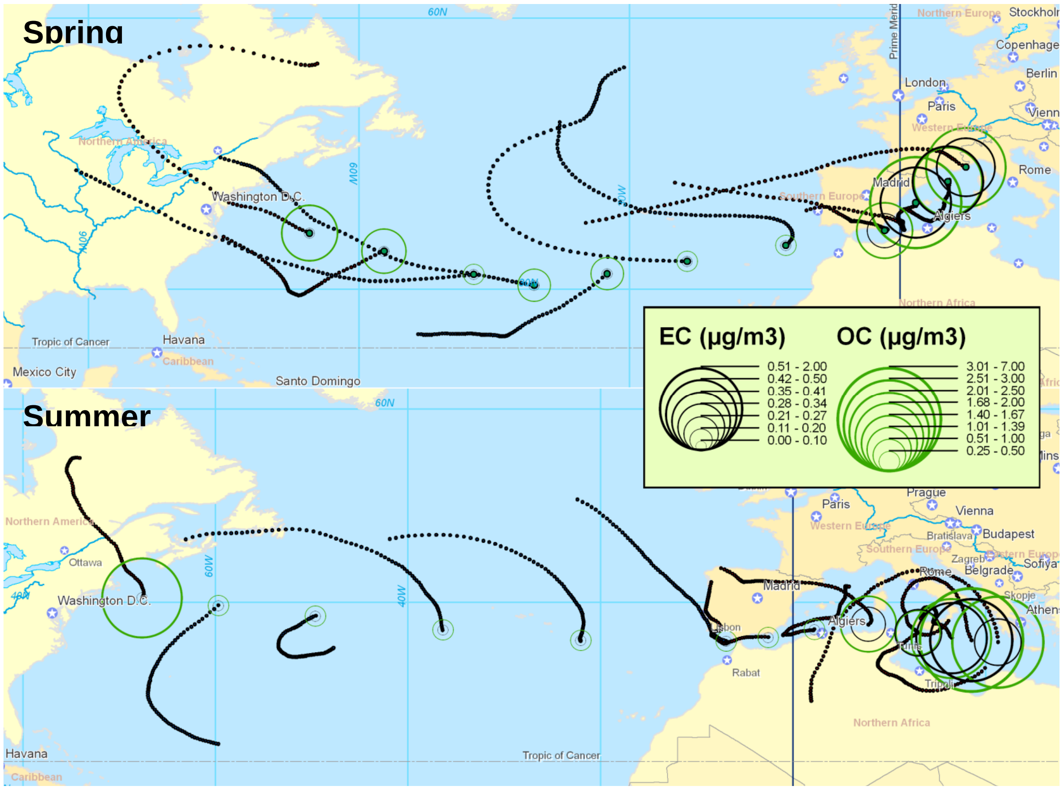

Figure 17. Organic (green) and elemental (black) carbon concentration of the particulate matter are shown for the E-W cruises. The black dots indicate the 72 hour air mass back-trajectories.

While organic carbon can be formed as a secondary product through gas phase oxidation, it is a primary product of anthropogenic and biogenic emissions. Since the open ocean would have negligible anthropogenic emissions it is not surprising that particulate samples, with air mass back-trajectories over a terrestrial environment and therefore passing over an area with higher anthropogenic inputs, would have a higher organic carbon concentration. Similarly, elemental carbon is a product of combustion and therefore will have a declining concentration as the sampling moved away from the combustion source, e.g., industrial combustion, transportation, or biomass burning.

4.1.2. Water-Soluble Organic Carbon and Total Dissolved Nitrogen

As previously mentioned, the water soluble fraction of the organic fraction was also calculated. Water soluble organic carbon (WSOC) is an important fraction of the OC because it affects the hygroscopicity of particles, which in turn affects the particles ability to form cloud condensation nuclei. Through its impact on cloud formation, WSOC has an indirect effect on climate.

In a previous study (Kondo et al., 2007), 88±29% of the oxygenated organic aerosol in Tokyo, Japan was attributed to WSOC and Miyazaki et al. (2006) found a correlation ($r^2 = 0.61$-0.79) between WSOC and secondary organic aerosol. These findings indicate that %WSOC can be used as a gauge for aged particulate, especially in an urban environment. Whether this is true for marine atmospheric particulate is unclear.

The WSOC in the atmospheric particulate samples, was found to be in higher concentration near the coast over the the open ocean. This suggests that the coastal sites have a more aged/oxidized component. Considering that the bulk of the organic carbonaceous material is coming from land (as seen in the higher OC concentration near the coast) and that the air mass does have to travel from the terrestrial source to the ship at sea; the particulate would potentially be more oxidized or "aged".

It has also been stated that WSOC is more closely associated with the SOA formed from anthropogenic VOC's (Sullivan and Weber, 2006). If this is the case, the higher WSOC in the coastal ocean samples may be due to the higher anthropogenic inputs from land.

Similarly, to OC, EC, and WSOC, the total dissolved nitrogen concentration in the water-soluble portion of the samples was higher in the coastal samples, then in the open ocean samples.

4.1.3. Size Exclusion Chromatography

The molecular size distribution of the water-soluble fraction of carbonaceous atmospheric particulate of a representative open and coastal ocean sample is compared to a standard of Suwannee River fulvic acid (SRFA) (Figure 18). SRFA was analyzed because of its use as a surrogate for atmospheric humic like substances (HULIS) (Arakaki et al., 2010; Chan and Chan, 2003), which are a class of organic compounds found in atmospheric particulate that share similarities to humic and fulvic acids found in terrestrial/aquatic environments. Most notable here, is the

SRFA standard consisting of one broad peak, whereas the atmospheric samples have multiple maxima. While this cause of the multiple peaks in the molecular size distribution of the atmospheric samples was not examined in the present study, it does create a question as to whether SRFA can be used as a model compound for studies regarding HULIS.

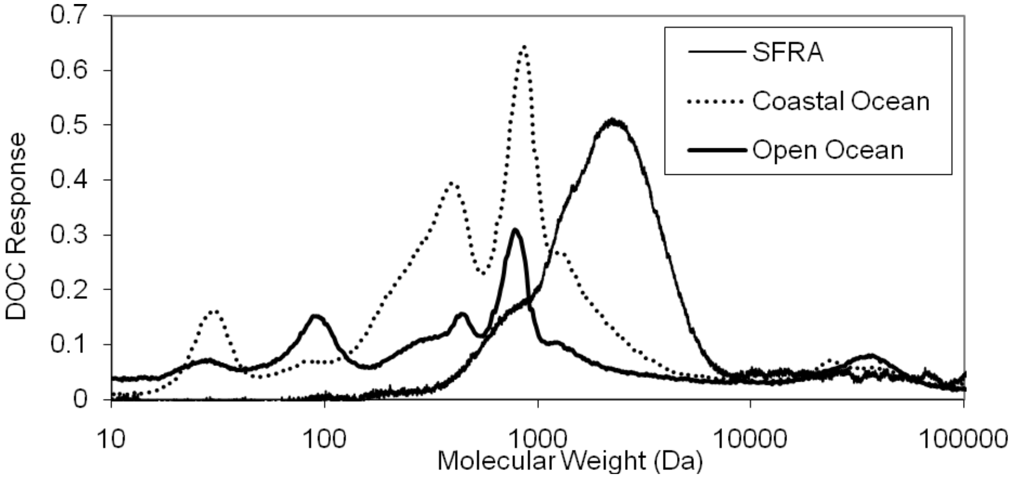

Figure 18. Comparison of the molecular size distribution of Suwannee River fulvic acid and representative (E-W transect) open and coastal ocean samples.

The difference between the open and coastal ocean representative samples (Figure 13, 18) is mainly with the lower molecular weight peak. The coastal ocean sample maxima occurs at approximately 30 Da (MW is based on PEG calibrations and, therefore, approximate), whereas the open ocean sample is slightly higher; approximately 100 Da. This area does fall below the lowest MW sample (200 Da) in the calibration curve, so the exact MW cannot be determined with any certainty. The cause of the smaller molecular size may be again caused by the anthropogenic input in the coastal samples. Atmospheric oxidation processes, as well as source combustion would lead to smaller molecular weight molecules. The higher percentage of WSOC in the coastal samples indicates more oxidized particles and the higher concentration of EC indicates increased combustion of the coastal samples over the open ocean.

4.1.4. Molecular Oxygenation and Saturation

In order to examine fully the differences in oxidation of atmospheric particulate with respect to location, previously analyzed samples from various locations, as well as the open and coastal ocean samples from figure 15, were plotted according to the ratio of the integrated area corresponding to the particular functional group (oxygenated aliphatic [H-C-O], unsaturated aliphatic groups [H-C=C], or saturated aliphatic groups [H-C]) to the sum of all integrated areas (Figure 19).

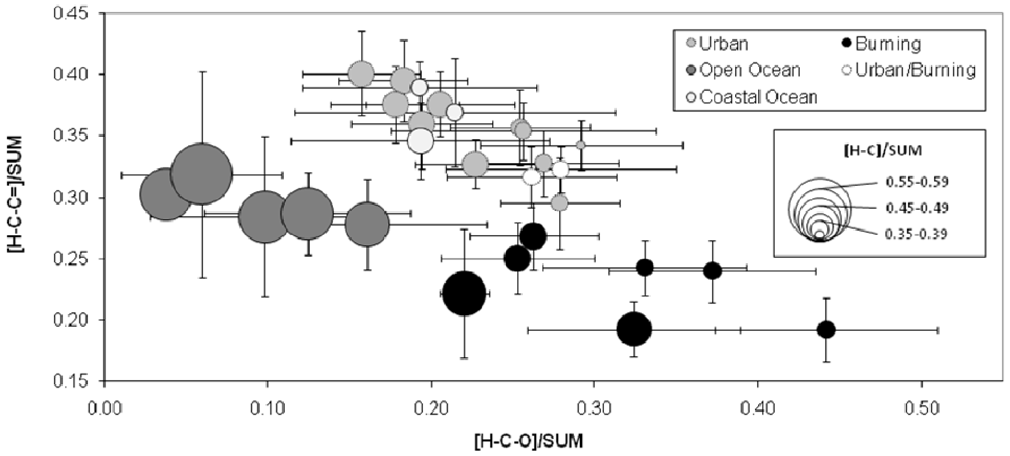

Figure 19. Index of oxygenation versus saturation of open ocean and coastal ocean samples. All values are the ratio of the integrated area corresponding to the particular functional group (oxygenated aliphatic [H-C-O], unsaturated aliphatics [H-C=C], or saturated aliphatics [H-C]) to the sum of all integrated areas.

The coastal locations contain a smaller concentration of saturated aliphatic groups and a larger concentration of oxygenated compounds (Figure 15, 29). This, coupled with the higher concentration of WSOC, indicates a particulate source of oxidized anthropogenic VOC's. Due to this, it is not unexpected that the coastal ocean samples show a closer relation to the urban samples in oxygenation and saturation (Figure 19). The open ocean samples, on the other hand, contained more saturated aliphatic groups and fewer oxygenated compounds, which agree with the WSOC data for that area. Airborne cellular material, such as lipids may be a source for the insoluble saturated aliphatic compounds. In fact, the only other samples that have comparable [H-C]/sum values are certain biomass burning samples. However, with the limited sample sets, it is difficult to draw any conclusions regarding their similarities.

A previous study (Decesari et al., 2007), indicated that urban areas contain a higher ratio of the aliphatic esters/ethers [H-C-O], than clean marine environments, which we see here (Figure 19). The samples collected during this North Atlantic study defined as coastal ocean show a larger ratio of [H-C-O] (Figure 15). Since these samples have a higher anthropogenic input, it is not surprising that they more closely resemble samples from an urban environment.

Due the small sample set, seasonal variations could not be considered.

4.2. Seasonal Differences in the Atmospheric Particulate Matter

The second part of this research examined the seasonal differences between the samples collected along the E-W transect in the North Atlantic Ocean.

4.2.1. Chlorophyll a and Fluorescence

It has been stated that the increase in OC in the open ocean samples during the spring cruise are linked to the seasonal location of marine phytoplankton blooms, which have been shown to peak in the north Atlantic in spring and decline (move north) in the summer (Cavalli et al., 2004; Yoon et al., 2007). To verify this, both satellite-derived concentrations of Chlorophyll a (Figure 20) and surface ocean fluorescence measurements, which are used as a proxy for the concentration marine phytoplankton, were analyzed.

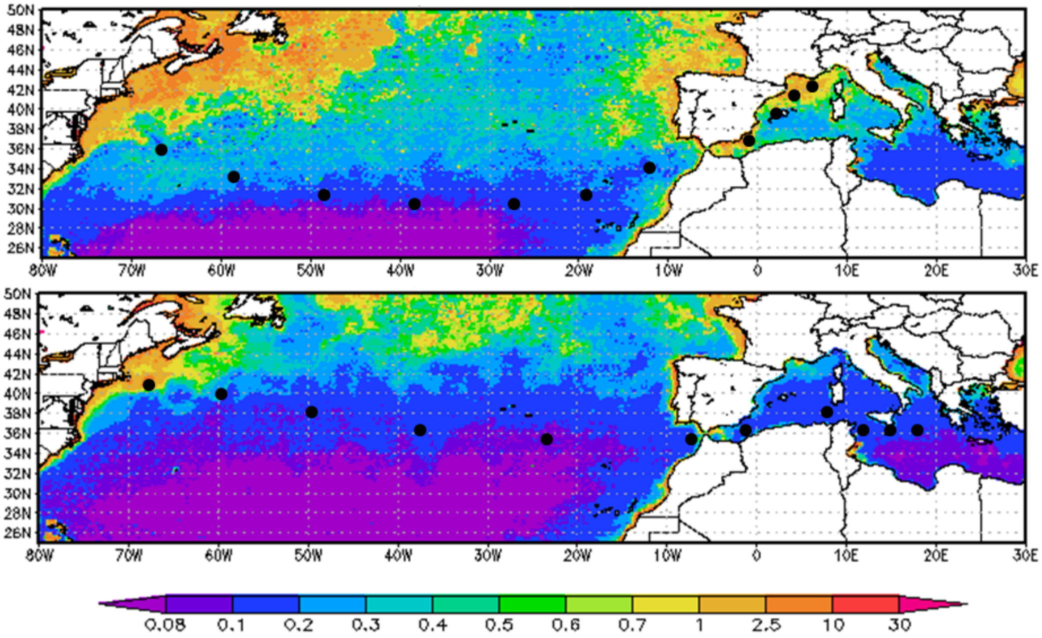

Figure 20. Chlorophyll a concentrations obtained from the SeaWiFS satellite.

Chlorophyll a concentrations derived from the satellite data, are higher in our sampling area on the coasts and out into the open ocean in the spring and decrease in these areas (move north) during the summer (Figure 20). This correlates with the decreased OC concentrations in the summer as compared to the spring.

The continuous fluorescence measurements taken of the ocean surface water during the two cruises found that the average 'open ocean' fluorescence measurements were significantly higher ($p<0.05$) during the spring cruise (Figure 21). This also agrees with an increase in marine productivity in the area during the spring, which coincides with the higher levels of OC during that time and indicates that there is a marine source for the organic carbon.

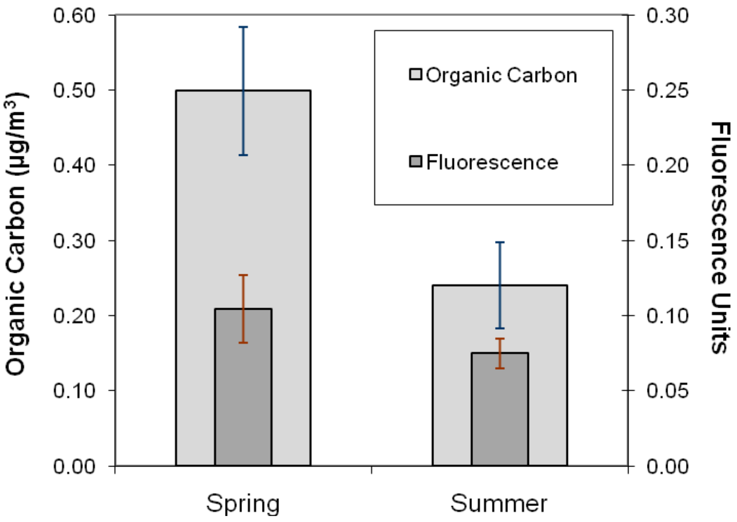

Figure 21. Average open ocean organic carbon concentrations and average surface ocean fluorescence concentrations for the spring and summer North Atlantic cruises. The differences are significant ($p<0.05$) in OC and fluorescence

4.2.2. Organic Carbon

The average OC for open ocean samples is 0.449 and 0.261 µg/m^3 for spring and summer, respectively. These OC concentrations are comparable to previous measurements in marine environments (Table 2), both falling within the OC measurements determined for the samples collected at Amsterdam Island (Sciare et al., 2009).

Organic particulate in the marine atmosphere is either transported from terrestrial environments or enters the atmosphere through bubble bursting/wind shear. After incorporation in the atmosphere, it will either exit via wet or dry deposition or be transformed through oxidative processes. Lim et al. (2003) found that EC has a longer atmospheric lifetime than OC and since EC is product of combustion and therefore primarily terrestrial in nature, marine samples were identified as open ocean, if they had EC concentrations below the detection limit. This implies that the source of the carbonaceous atmospheric particulate in the open ocean samples is the ocean itself. More specifically, it is the surface layer that is ejected into the atmosphere via bubble bursting/wind shear. For this reason, it was hypothesized that the organic carbon concentration would increase in atmospheric particulate collected in the open ocean if

Table 2
OC and EC measurements collected in marine environments.

Location	OC (µg/m^3)	EC (µg/m^3)
Cape San Juan, Puerto Rico *(Novakov et al., 1997)*	0.391	
Tenerife Island (28°18'N, 16°30'W) *(Putaud et al., 2000)*	0.210	
Azores (38°41'N,27°21'W) Summer *(Pio et al., 2007)*	0.380	0.047
Azores (38°41'N,27°21'W) Winter *(Pio et al., 2007)*	0.270	0.039
Amsterdam Island (37°31'S,77°19'E) *(Sciare et al., 2009)*	0.037-0.530	BDL-0.062
North Atlantic Open Ocean Spring Transect Average	0.449	<0.015
North Atlantic Open Ocean Summer Transect Average	0.261	<0.015

the organic carbon concentration of the surface layer of the ocean increased; namely the annual phytoplankton bloom, which peaks in the early spring and declines into the summer.

The difference between the spring and summer average OC concentrations (0.449 and 0.261 $\mu g/m^3$, respectively) was found to be statistically significant ($p<0.05$). This increased organic carbon concentration in spring followed by a decrease in summer agrees with findings from the Mace Head Atmospheric Research Station, where “clean” North Atlantic air masses exhibited a similar seasonal pattern (Yoon et al., 2007) attributed to a biogenic marine source. A seasonal pattern was also observed in samples collected on Amsterdam Island (Sciare et al., 2009), where an increase in OC coincided with high marine productivity.

4.2.3. Water-Soluble Organic Carbon

The percent water-soluble organic carbon shows no statistically significant difference between the spring and summer sampling events. Percent WSOC has been shown to be highly correlated with oxygenated OC (Kondo et al., 2007), which is closely linked with anthropogenic SOA (Miyazaki et al., 2006). For this reason, finding discernable differences in the %WSOC between the two seasons was not expected.

Examination of the water-insoluble organic carbon (WIOC) portion of the open ocean particulate, however, did show a significant difference ($p<0.05$) between the spring (0.35 $\mu g/m^3$) and summer (0.20 $\mu g/m^3$). An increase in WIOC during the spring may be caused by the increase in insoluble cellular material such as lipids and other long chain alkanes. In fact, Facchini et al. (2008) found that the OC associated with bubble bursting events was primarily insoluble during the North Atlantic phytoplankton bloom. This increase in WIOC during peak biogenic activity also agrees with previous studies in the North Atlantic (Cavalli et al., 2004; O'Dowd et al., 2004; Yoon et al., 2007).

4.2.4. Size Exclusion Chromatography

Overall atmospheric processes tend to break down organic matter through oxidation. Therefore, it is likely that samples collected during a period of increased primary emissions, would have a higher average molecular weight. If higher biogenic primary emission, via bubble bursting, occurs during peak phytoplankton periods, one would expect to see changes in the DOC response due to seasonal variability in phytoplankton productivity.

A plot of the molecular size distribution of the water-soluble organic compounds of representative spring and summer open ocean samples is shown in figure 15. Both samples have a maximum peak below 1000 Da, but the plot of the summer sample is down shifted to lower MW’s, which increases in magnitude as the MW decreases. Exact MW data below 200 Da is uncertain, since this falls below the calibration curve, however, the summer sample does show a larger fraction of the WSOC coming from smaller molecules in the summer.

If we assume the hypothesis that lower biogenic marine production would lead to a lower concentration in primary emissions from the ocean surface, then a larger portion of the atmospheric particulate during these times would be aged emissions from downwind. Therefore, the summer atmospheric particulate over the open ocean would contain a larger percentage of oxidized molecules and would be smaller in size.

The summer sample also differed from the spring in the very high MW region (~40,000 Da). This peak in the summer sample is over 3 times that of the spring sample. A previous study of wastewater effluent (Song et al., 2010) attributes SEC-DOC peaks >10 kDa to organic colloids. The C/N ratio found in these colloids was slightly lower than that found in the surface water of the Mid-Atlantic Bight (Santschi et al., 1998); 6.2 and 11, respectively. The TEM images of the organic colloids in the effluent, however, show long fibrils similar in shape and size to the colloids of the surface waters studied by Santshci et al (1998).

The increase during the summer of these organic colloids is unknown. However, an increase in organic matter in the marine surface water during the phytoplankton bloom may cause colloidal material, which tends to aggregate (Santschi et al., 1998), to remain in the surface marine layer instead of being ejected during bubble bursting. Then, when the bloom subsides during the summer and the organic matter decreases in the marine surface layer, the less aggregated colloidal material can be ejected and become part of the atmospheric particulate.

5. Conclusions

Using a variety of methods to analyze bulk carbon characteristics - thermal optical transmittance, non-purgeble organic carbon analysis, size exclusion chromatography, nuclear magnetic resonance –variation in shipboard atmospheric particulate matter samples, with regard to location and season, was found over the North Atlantic Ocean.

5.1. Open versus Coastal Ocean Sampling Locations

Analysis of the marine samples showed clear difference in the concentrations of OC, EC, and WSOC between the coastal and open ocean. The coastal ocean had higher concentrations in all three carbonaceous particulate subsets. The 72-hour air mass back-trajectories of the coastal samples indicate that terrestrial inputs were most likely the cause of this. The higher concentration of WSOC in the coastal sites suggests that the particulate has a more aged/oxidized component. Considering that the bulk of the carbonaceous material is coming from land and that the air mass does have to travel from the terrestrial source to the ship at sea; the large portion of the particulate would be more oxidized.

The functional group content of the particulate in the atmosphere also showed some differences. The open ocean samples contained more saturated aliphatics and fewer oxygenated compounds which may be why they are less water soluble. Lipids, from possible airborne cellular material, could lead to the increase in insoluble saturated aliphatic compounds. The coastal locations contained small amounts of saturated aliphatics and larger amounts of oxygenated compounds, which could be caused by the samples being of terrestrial origin, but more aged in nature due to the distance from shore travelled.

5.2. Seasonal Variation in Carbonaceous Particulate Matter

Seasonal variations of the open ocean sample concentrations were compared between the two cruises (spring and summer). Spring samples (March-April) were found to have a significantly ($p<0.05$) increased organic carbon concentration over the summer (June-July) samples. This was analyzed along with the Chlorophyll a and fluorescence concentrations. The SeaWiFs Chlorophyll a data suggested that the marine phytoplankton population was larger in the spring than in the summer for the sampling locations in the North Atlantic, and the fluorescence data indicates a significant ($p<0.05$) increase in Chlorophyll a concentration during the spring. This agrees with the previous theory (O'Dowd et al., 2004) that atmospheric particulate over marine environments can be significantly affected by biogenic inputs.

The percent water soluble organic carbon (WSOC) of organic carbon (OC), however, did not show any significant differences and is, therefore, inconclusive. When examining the size distribution of the water soluble portion, though, the spring samples generally had a higher molecular weight (MW), with the exception of the broad peak (~40,000 Da). The higher MW in the spring may be a function of a primary source being less oxidized. The lack of the highest MW peak may be caused by the bloom phytoplankton being too large to remain in the atmospheric particulate. Conversely, the summer appears to have a lower MW with the exception of the high MW broad peak (~40,000 Da). It has been suggested that peaks in this size range can be caused by nanoscale colloids which, in this case, could be biogenic colloids. Further study would need to be done to examine this hypothesis.

5.3. Future Outlook

First, in order to draw more detailed conclusions on the role marine life plays in the ocean atmosphere, more samples will need to be collected over multiple seasons, especially collection with a larger seasonal gap, i.e. winter versus summer or spring versus autumn. A positive correlation between OC and phytoplankton activity in the open ocean would further support the conclusions that marine productivity has a considerable affect on the atmospheric particulate matter.

Second, it would be useful to separate the atmospheric particulate samples into molecular weight size fractions, using size exclusion chromatography, for a more detailed analysis. The chosen size fractions could be analyzed for specific compounds or groups of compounds. For instance, the broad molecular weight peak (~40,000 Da) could be analyzed for cellular tracers. Through this analysis, a clearer understanding could be gained of the ocean's impact on the surrounding atmospheric particulate.

REFERENCES

A. Andracchio, C. Cavicchi, D. Tonelli and S. Zappoli, A new approach for the fractionation of water-soluble organic carbon in atmospheric aerosols and cloud drops, *Atmospheric Environment* **36**(2002), pp. 5097-5107.

T. Arakaki, K. Saito, K. Okada, H. Nakajima and Y. Hitomi, Contribution of fulvic acid to the photochemical formation of Fe(II) in acidic Suwannee River fulvic acid solutions, *Chemosphere* **78**(2010), pp. 1023-1027.

H.P.H. Arp, R.P. Schwarzenbach and K.U. Goss, Equilibrium sorption of gaseous organic chemicals to fiber filters used for aerosol studies, *Atmospheric Environment* **41**(2007), pp. 8241-8252.

D.C. Blanchard, The electrification of the atmosphere by particles from bubbles in the sea, *Progress In Oceanography* **1**(1963), p. 73.

D.C. Blanchard, The Production, Distribution, and Bacterial Enrichment of the Sea-Salt Aerosol. In: P.S. Liss and W.G.N. Slinn, Editors, *Air-Sea Exchange of Gases and Particles*, D. Reidel Publishing Company, Dordrecht, Holland (1982).

C. Bowler and P. Brimblecombe, ARCHIVES AND AIR-POLLUTION HISTORY, *J. Soc. Arch.* **13**(1992), pp. 136-142.

P. Brimblecombe, INTEREST IN AIR-POLLUTION AMONG EARLY FELLOWS OF ROYAL SOCIETY, *Notes Rec. R. Soc. Lond.* **32**(1978), pp. 123-129.

P. Bruice, *Organic Chemistry*, 3rd ed, Prentice Hall, New Jersey (2001).

P. Buat-Menard, Particle Geochemistry in the Atmosphere and Oceans. In: P.S. Liss and W.G.N. Slinn, Editors, *Air-Sea Exchange of Gases and Particles*, D. Reidel Publishing Company, Dordrecht, Holland (1983).

Ø. Buhaug *et al.*, Second IMO GHG Study 2009. International Maritime Organization (IMO), London, UK (2009).

K.S. Carslaw *et al.*, A review of natural aerosol interactions and feedbacks within the Earth system, *Atmospheric Chemistry And Physics* **10**(2010), pp. 1701-1737.

F. Cavalli *et al.*, Advances in characterization of size-resolved organic matter in marine aerosol over the North Atlantic, *Journal Of Geophysical Research-Atmospheres* **109**(2004).

M.N. Chan and C.K. Chan, Hygroscopic properties of two model humic-like substances and their mixtures with inorganics of atmospheric importance, *Environmental Science & Technology* **37**(2003), pp. 5109-5115.

R.J. Charlson and J. Heintzenberg, *Aerosol Forcing of Climate*, John Wiley & Sons Ltd, Chichester (1995) 416 pp.

S. Decesari *et al.*, Source attribution of water-soluble organic aerosol by nuclear magnetic resonance spectroscopy, *Environmental Science & Technology* **41**(2007), pp. 2479-2484.

M.C. Facchini *et al.*, Primary submicron marine aerosol dominated by insoluble organic colloids and aggregates, *Geophys. Res. Lett.* **35**(2008).

B.J. Finlayson-Pitts and J.N. Pitts, *Chemistry of the Upper and Lower Atmosphere*, Academic Press, San Diego, CA (2000).

A. Gelencser, *Carbonaceous Aerosol*, Springer, Dordrecht, The Netherlands (2004) 350 pp.

R. Gioia *et al.*, Polychlorinated biphenyls in air and water of the North Atlantic and Arctic Ocean, *Journal Of Geophysical Research-Atmospheres* **113**(2008), p. 11.

N. Her *et al.*, Optimization of method for detecting and characterizing NOM by HPLC-size exclusion chromatography with UV and on-line DOC detection, *Environmental Science & Technology* **36**(2002a), pp. 1069-1076.

N. Her, G. Amy, D. Foss and J.W. Cho, Variations of molecular weight estimation by HP-size exclusion chromatography with UVA versus online DOC detection, *Environmental Science & Technology* **36**(2002b), pp. 3393-3399.

IPCC, Climate Change 2007: Synthesis Report. Contribution of Working Groups I, II and III to the Fourth Assessment Report of the Intergovernmental Panel on Climate Change. In: C.W. Team, R.K. Pachauri and A. Reisinger, Editors, Geneva, Switzerland (2007), p. 104.

Y. Kondo *et al.*, Oxygenated and water-soluble organic aerosols in Tokyo, *Journal Of Geophysical Research-Atmospheres* **112**(2007).

Z. Krivacsy *et al.*, Study of humic-like substances in fog and interstitial aerosol by size-exclusion chromatography and capillary electrophoresis, *Atmospheric Environment* **34**(2000), pp. 4273-4281.

J.H. Kroll and J.H. Seinfeld, Chemistry of secondary organic aerosol: Formation and evolution of low-volatility organics in the atmosphere, *Atmospheric Environment* **42**(2008), pp. 3593-3624.

A.A. Lacis and M.I. Mishchenko, Climate Forcing, Climate Sensitivity, and Climate Response: A Radiative Modeling Perspective on Atmospheric Aerosols. In: C. R.J. and J. Heintzenberg, Editors, *Aerosol Forcing of Climate*, John Wiley & Sons Ltd., Chichester (1995), p. 416.

H.J. Lim, B.J. Turpin, L.M. Russell and T.S. Bates, Organic and elemental carbon measurements during ACE-Asia suggest a longer atmospheric lifetime for elemental carbon, *Environmental Science & Technology* **37**(2003), pp. 3055-3061.

R. Lohmann *et al.*, Organochlorine Pesticides and PAHs in the Surface Water and Atmosphere of the North Atlantic and Arctic Ocean, *Environmental Science & Technology* **43**(2009), pp. 5633-5639.

Y. Mamane, Air Pollution Control in Isreal During the First and Second Century, *Atmospheric Environment* **21**(1987), p. 3.

S.F. Maria, L.M. Russell, B.J. Turpin and R.J. Porcja, FTIR measurements of functional groups and organic mass in aerosol samples over the Caribbean, *Atmospheric Environment* **36**(2002), pp. 5185-5196.

Y. Miyazaki *et al.*, Time-resolved measurements of water-soluble organic carbon in Tokyo, *Journal Of Geophysical Research-Atmospheres* **111**(2006).

S.N. Nam and G. Amy, Differentiation of wastewater effluent organic matter (EfOM) from natural organic matter (NOM) using multiple analytical techniques, *Water Sci. Technol.* **57**(2008), pp. 1009-1015.

L. Nizzetto *et al.*, PAHs in air and seawater along a North-South Atlantic transect: Trends, processes and possible sources, *Environmental Science & Technology* **42**(2008), pp. 1580-1585.

T. Novakov *et al.*, Organic aerosols in the Caribbean trade winds: A natural source?, *Journal Of Geophysical Research-Atmospheres* **102**(1997), pp. 21307-21313.

C.D. O'Dowd *et al.*, Biogenically driven organic contribution to marine aerosol, *Nature* **431**(2004), pp. 676-680.

C.D. Odowd, M.H. Smith and S.G. Jennings, Submicron Particle, Radon, And Soot Carbon Characteristics Over The Northeast Atlantic, *Journal Of Geophysical Research-Atmospheres* **98**(1993), pp. 1123-1135.

C.A. Pio *et al.*, Climatology of aerosol composition (organic versus inorganic) at nonurban sites on a west-east transect across Europe, *Journal Of Geophysical Research-Atmospheres* **112**(2007), p. 15.

R. Pueschel, *Composition Chemistry, and Climate of the Atmosphere*, Van Nostrand Reinhold, New York (1995) 527 pp.

J.P. Putaud *et al.*, Chemical mass closure and assessment of the origin of the submicron aerosol in the marine boundary layer and the free troposphere at Tenerife during ACE-2, *Tellus Series B-Chemical and Physical Meteorology* **52**(2000), pp. 141-168.

P.K. Quinn and T.S. Bates, Regional aerosol properties: Comparisons of boundary layer measurements from ACE 1, ACE 2, aerosols99, INDOEX, ACE asia, TARFOX, and NEAQS, *Journal Of Geophysical Research-Atmospheres* **110**(2005).

H.J. Reich, Proton Chemical Shifts. Department of Chemistry, University of Wisconsin (2011).

Y. Rudich, N.M. Donahue and T.F. Mentel, Aging of organic aerosol: Bridging the gap between laboratory and field studies, *Annu. Rev. Phys. Chem.* **58**(2007), pp. 321-352.

V. Samburova *et al.*, Seasonal variation of high-molecular-weight compounds in the water-soluble fraction of organic urban aerosols, *Journal Of Geophysical Research-Atmospheres* **110**(2005).

P.H. Santschi *et al.*, Fibrillar polysaccharides in marine macromolecular organic matter as imaged by atomic force microscopy and transmission electron microscopy, *Limnol. Oceanogr.* **43**(1998), pp. 896-908.

R.E. Schwartz *et al.*, Biogenic oxidized organic functional groups in aerosol particles from a mountain forest site and their similarities to laboratory chamber products, *Atmospheric Chemistry And Physics* **10**(2010), pp. 5075-5088.

J. Sciare *et al.*, Long-term observations of carbonaceous aerosols in the Austral Ocean atmosphere: Evidence of a biogenic marine organic source, *Journal Of Geophysical Research-Atmospheres* **114**(2009).

H.K. Shon, S.H. Kim, L. Erdei and S. Vigneswaran, Analytical methods of size distribution for organic matter in water and wastewater, *Korean J. Chem. Eng.* **23**(2006), pp. 581-591.

G.X. Song, J. Wang, C.A. Chiu and P. Westerhoff, Biogenic Nanoscale Colloids in Wastewater Effluents, *Environmental Science & Technology* **44**(2010), pp. 8216-8222.

D.E. Speil, The Droplets Produced by Individual Bubbles Bursting on a Sea Water Surface. In: G.L. Geernaert, Editor, *Air-Sea Exchange: Physics, Chemistry and Dynamics*, Kluwer Academic Publishers, Dordrecht, Holland (1999).

R. Subramanian, A.Y. Khlystov, J.C. Cabada and A.L. Robinson, Positive and Negative Artifacts in Particulate Organic Carbon Measurements with Denuded and Undenuded Sampler Configurations -- of <i>Aerosol Science and Technology</i> on Findings from the Fine Particulate Matter Supersites Program, *Aerosol Sci. Technol.* **38**(2004), pp. 27 - 48.

A.P. Sullivan and R.J. Weber, Chemical characterization of the ambient organic aerosol soluble in water: 2. Isolation of acid, neutral, and basic fractions by modified size-exclusion chromatography, *Journal Of Geophysical Research-Atmospheres* **111**(2006).

R.L. Tanner, W.J. Parkhurst, M.L. Valente and W. David Phillips, Regional composition of PM2.5 aerosols measured at urban, rural and "background" sites in the Tennessee valley, *Atmospheric Environment* **38**(2004), p. 3143.

B.J. Turpin, J.J. Huntzicker and S.V. Hering, Investigation of organic aerosol sampling artifacts in the los angeles basin, *Atmospheric Environment* **28**(1994), p. 3061.

C.A. Tyree, Size and Composition of Foam Droplets with Applications to the Marine Atmosphere and Nanoparticle Synthesis. Arizona State University, Tempe (2007), p. 179.

M. Viana *et al.*, Comparative analysis of organic and elemental carbon concentrations in carbonaceous aerosols in three European cities, *Atmospheric Environment* **41**(2007), pp. 5972-5983.

B. Warton, A. Heitz, B. Allpike and R. Kagi, Size-exclusion chromatography with organic carbon detection using a mass spectrometer, *J. Chromatogr. A* **1207**(2008), pp. 186-189.

Y.J. Yoon *et al.*, Seasonal characteristics of the physicochemical properties of North Atlantic marine atmospheric aerosols, *Journal Of Geophysical Research-Atmospheres* **112**(2007).

K.E. Yttri *et al.*, Elemental and organic carbon in PM10: a one year measurement campaign within the European Monitoring and Evaluation Programme EMEP, *Atmospheric Chemistry And Physics* **7**(2007), pp. 5711-5725.

K.E. Yttri, C. Dye, O.A. Braathen, D. Simpson and E. Steinnes, Carbonaceous aerosols in Norwegian urban areas, *Atmospheric Chemistry And Physics* **9**(2009), pp. 2007-2020.

L. Zhang and R. Lohmann, Cycling of PCBs and HCB in the Surface Ocean-lower Atmosphere of the Open Pacific, *Environmental Science & Technology* **44**(2010), pp. 3832-3838.

APPENDIX A

Organic, Elemental, and Total Carbon Concentration Data for Samples Collected during the North-South and both East-West Transects

OC, EC, and TC concentration for samples collected during the N-S transect. Values below the detection limit (15 ng/mL) are indicated by BDL.

Latitude	Longitude	Organic Carbon (μg/m^3)	Elemental Carbon (μg/m^3)	Total Carbon (μg/m^3)
49.9185	-3.1463	6.89	2.00	8.89
48.0485	-5.5685	2.83	0.53	3.36
46.4020	-5.9180	1.77	0.25	2.03
37.8640	-11.7957	0.60	0.20	0.80
30.4410	-16.3862	0.45	BDL	0.46
28.2505	-15.3813	0.32	BDL	0.32
24.6700	-18.8169	0.62	BDL	0.61
19.0927	-20.9107	0.89	0.15	1.04
17.1947	-20.9498	1.31	0.20	1.51
14.5334	-20.9538	1.52	0.12	1.63
12.4824	-20.5201	1.79	0.22	2.01
10.6228	-20.1312	1.72	0.48	2.20
7.6091	-17.9882	0.91	0.29	1.20
6.1176	-16.7393	1.19	0.29	1.48
2.9620	-14.1095	0.50	0.18	0.68
1.0303	-12.6065	0.51	0.21	0.72
-0.4904	-11.4240	0.53	0.11	0.64
-1.4338	-10.6905	0.76	0.05	0.81
-2.8478	-9.5900	0.69	0.07	0.76
-4.7634	-8.0973	0.55	BDL	0.55
-6.4281	-6.7966	0.72	BDL	0.73
-8.1268	-5.4650	0.35	0.03	0.38
-9.3918	-4.4699	0.47	0.02	0.49
-11.5601	-2.7553	0.43	0.04	0.47
-11.8633	-2.5140	0.42	BDL	0.42
-13.6215	-1.1129	0.55	0.13	0.68
-17.1201	1.7082	0.60	BDL	0.61
-18.5516	2.8784	0.44	BDL	0.44
-20.5077	4.4919	0.47	BDL	0.47
-23.8737	7.3190	0.58	0.02	0.59
-24.9520	8.2402	0.71	BDL	0.72

OC, EC, and TC concentration for samples collected during the spring E-W transect. Values below the detection limit (15 ng/mL) are indicated by BDL.

Latitude	Longitude	Organic Carbon (μg/m^3)	Elemental Carbon (μg/m^3)	Total Carbon (μg/m^3)
36.2300	-65.5000	1.64	0.08	1.72
34.2300	-57.2600	1.14	0.07	1.20
31.6600	-47.2900	0.45	BDL	0.45
30.4500	-40.5800	0.62	BDL	0.62
31.7400	-32.5100	0.50	BDL	0.51
33.1000	-23.6200	0.42	BDL	0.43
34.8800	-12.6900	0.25	BDL	0.25
36.5100	-1.7400	1.46	0.26	1.72
39.5900	1.7000	2.53	0.41	2.94
41.9300	5.2800	1.88	0.48	2.35
43.5400	7.2800	2.08	0.40	2.49

OC, EC, and TC concentration for samples collected during the summer E-W transect. Values below the detection limit (15 ng/mL) are indicated by BDL.

Latitude	Longitude	Organic Carbon (μg/m^3)	Elemental Carbon (μg/m^3)	Total Carbon (μg/m^3)
35.8684	21.2694	3.04	0.31	3.35
36.1008	18.5180	6.23	1.82	8.05
36.2821	16.4556	2.76	0.54	3.31
36.8535	12.9870	1.61	0.39	2.00
37.7461	7.8222	1.79	0.29	2.09
37.1840	2.1992	0.93	0.04	0.97
36.3658	-2.5889	0.70	0.06	0.76
35.9787	-6.9715	0.35	BDL	0.35
36.0309	-22.0601	0.19	BDL	0.19
37.1201	-36.3892	0.30	BDL	0.30
38.5550	-49.6178	0.19	BDL	0.20
39.6616	-59.6924	0.27	BDL	0.27
40.4899	-67.6350	2.78	0.05	2.83

APPENDIX B

Water-Soluble Organic Carbon and Total Dissolved Nitrogen Concentration Data for Samples Collected during the North-South and both East-West Transects; Water-Insoluble Organic Carbon Concentration Data for Samples Collected during both East-West Transects

WSOC and TDN concentration for samples collected during the N-S transect.

Latitude	Longitude	Water-Soluble Organic Carbon (µg/m^3)	Total Dissolved Nitrogen (µg/m^3)
49.9185	-3.1463	2.71	10.81
48.0485	-5.5685	1.20	1.73
46.4020	-5.9180	1.01	0.86
37.8640	-11.7957	0.43	0.65
30.4410	-16.3862	0.36	0.10
28.2505	-15.3813	0.29	0.06
24.6700	-18.8169	0.60	0.07
19.0927	-20.9107	0.23	0.19
17.1947	-20.9498	0.59	0.43
14.5334	-20.9538	1.10	0.49
12.4824	-20.5201	1.43	0.66
10.6228	-20.1312	1.32	0.81
7.6091	-17.9882	0.65	0.24
6.1176	-16.7393	0.61	0.07
2.9620	-14.1095	0.23	0.09
-1.4338	-10.6905	0.57	0.05
-2.8478	-9.5900	0.81	0.01
-4.7634	-8.0973	0.55	0.00
-6.4281	-6.7966	0.61	0.08
-9.3918	-4.4699	0.72	0.15
-11.5601	-2.7553	0.68	0.06
-13.6215	-1.1129	0.71	-0.02
-20.5077	4.4919	0.37	-0.03
-23.8737	7.3190	0.80	0.03

WSOC, TDN, and WIOC concentrations for samples collected during the spring E-W transect.

Latitude	Longitude	Water-Soluble Organic Carbon (µg/m^3)	Total Dissolved Nitrogen (µg/m^3)	Water-Insoluble Organic Carbon (µg/m^3)
36.2300	-65.5000	0.64	1.20	1.00
34.2300	-57.2600	0.55	0.33	0.59
31.6600	-47.2900	0.08	0.08	0.37
30.4500	-40.5800	0.12	0.17	0.50
31.7400	-32.5100	0.22	0.18	0.28
33.1000	-23.6200	0.07	0.10	0.35
34.8800	-12.6900	0.02	0.21	0.23
36.5100	-1.7400	0.91	1.75	0.56
39.5900	1.7000	1.45	1.92	1.12
41.9300	5.2800	1.20	1.91	0.68
43.5400	7.2800	1.20	0.86	0.88

WSOC, TDN, and WIOC concentrations for samples collected during the summer E-W transect.

Latitude	Longitude	Water-Soluble Organic Carbon ($\mu g/m^3$)	Total Dissolved Nitrogen ($\mu g/m^3$)	Water-Insoluble Organic Carbon ($\mu g/m^3$)
35.8684	21.2694	2.64	2.45	0.40
36.1008	18.5180	3.06	2.69	3.17
36.2821	16.4556	1.39	3.21	1.37
36.8535	12.9870	0.80	1.36	0.81
37.7461	7.8222	1.16	1.04	0.63
37.1840	2.1992	0.84	1.33	0.08
36.3658	-2.5889	0.39	0.59	0.30
35.9787	-6.9715	0.04	0.21	0.30
36.0309	-22.0601	0.02	0.09	0.17
37.1201	-36.3892	0.16	0.10	0.15
38.5550	-49.6178	0.02	0.09	0.18
39.6616	-59.6924	0.06	0.11	0.21
40.4899	-67.6350	1.83	0.31	0.95

APPENDIX C

Molecular Weight Distribution Data for Samples Collected during both East-West Transects

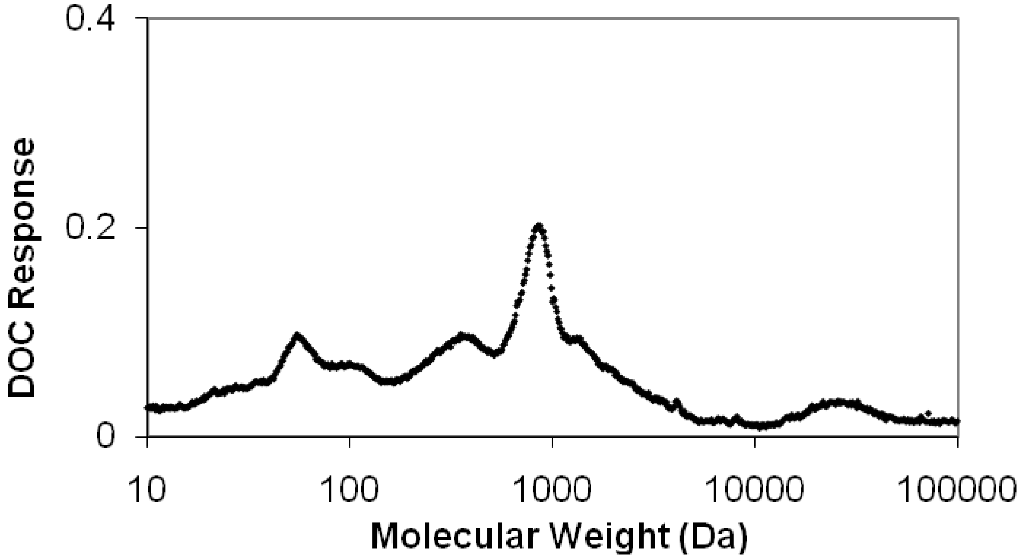

Spring East-West transect (36.2300, -65.5000).

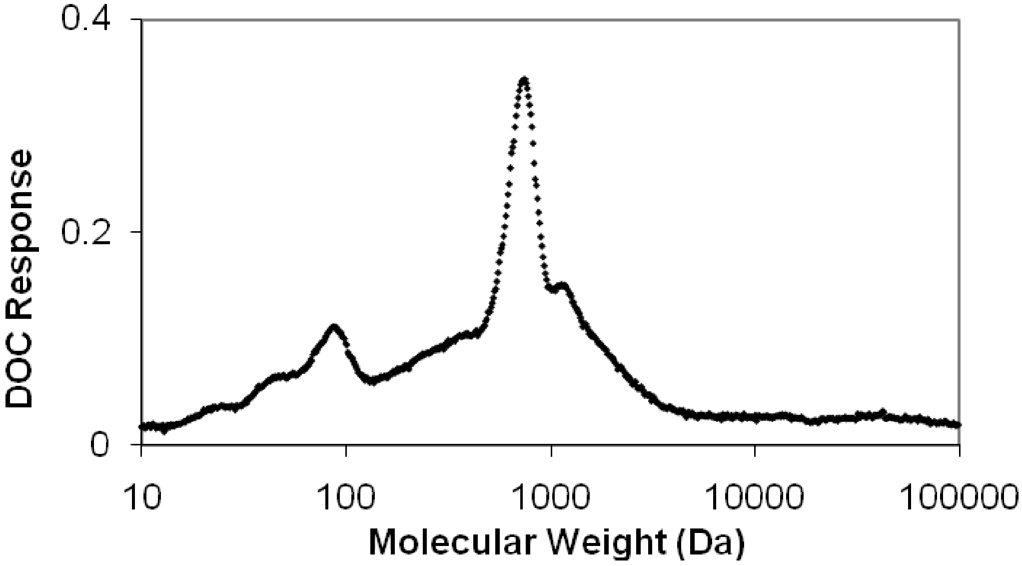

Spring East-West transect (34.2300, -57.2600).

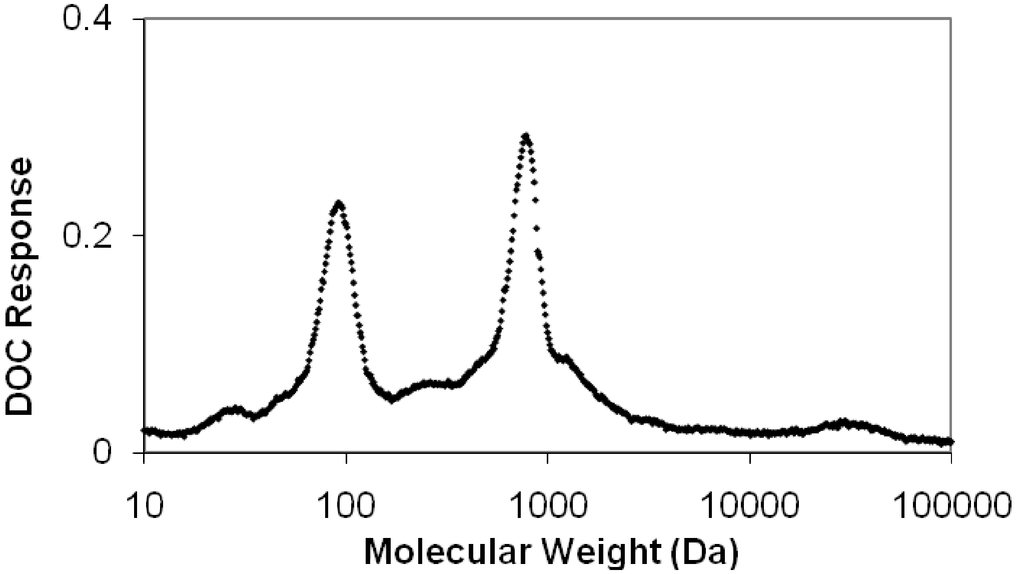

Spring East-West transect (31.6600, -47.2900).

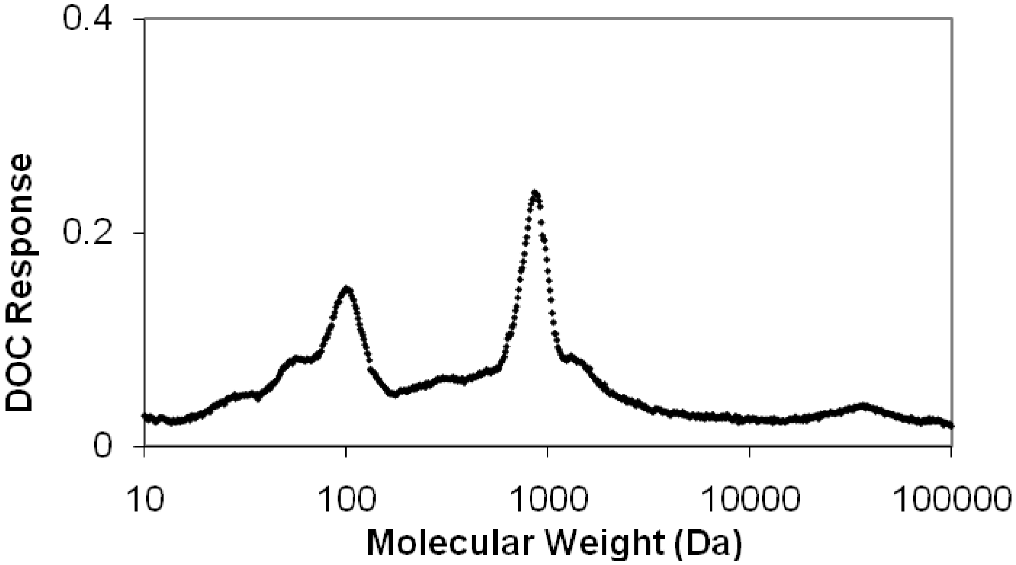

Spring East-West transect (30.4500, -40.5800).

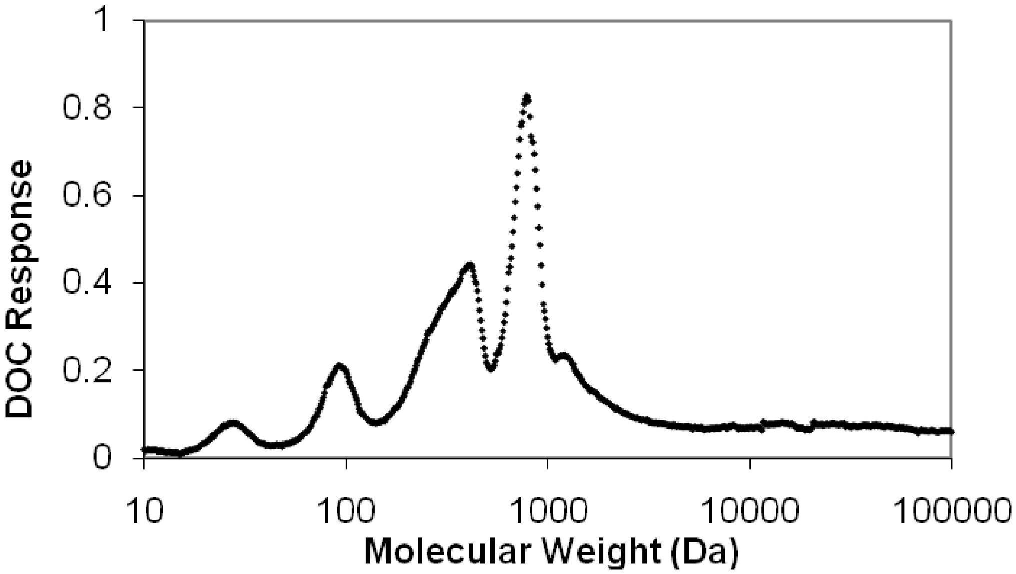

Spring East-West transect (31.7400, -32.5100).

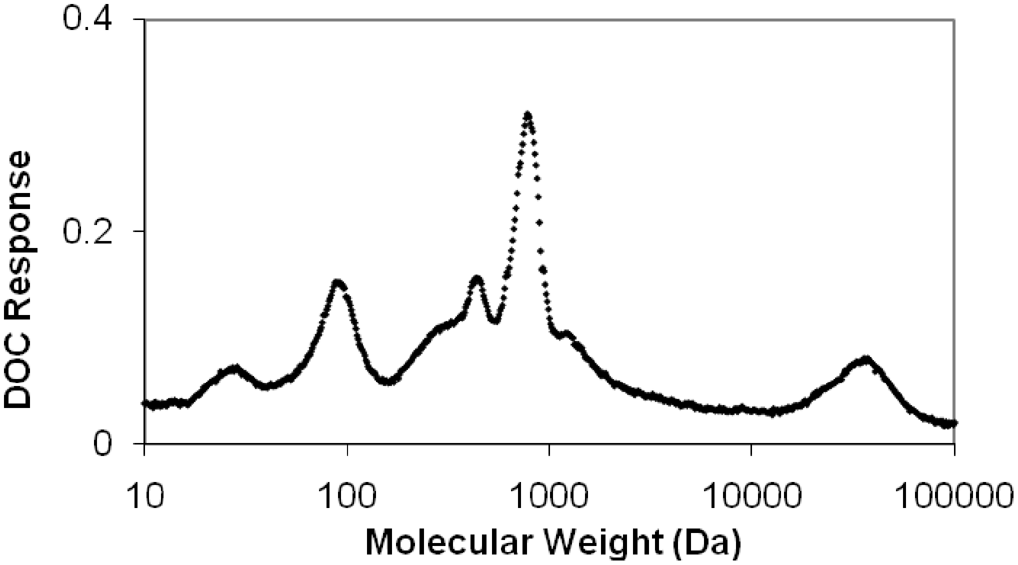

Spring East-West transect (33.1000, -23.6200).

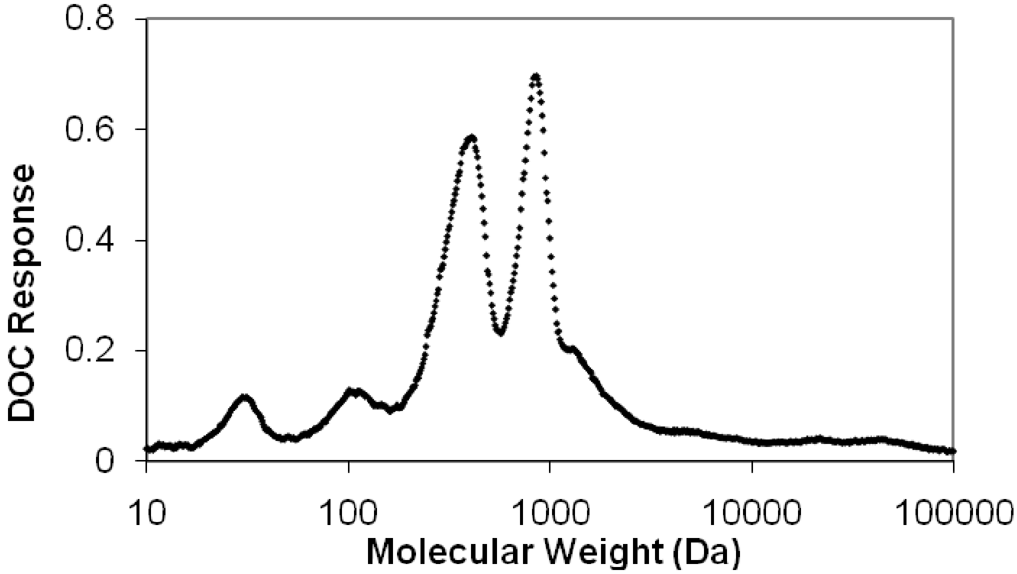

Spring East-West transect (34.8800, -12.6900).

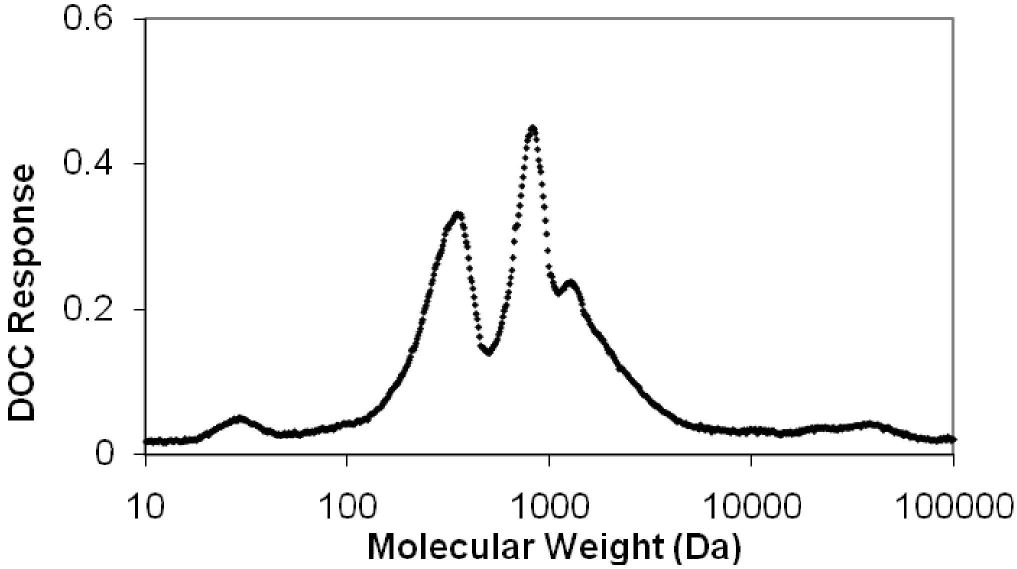

Spring East-West transect (39.5900, 1.7000).

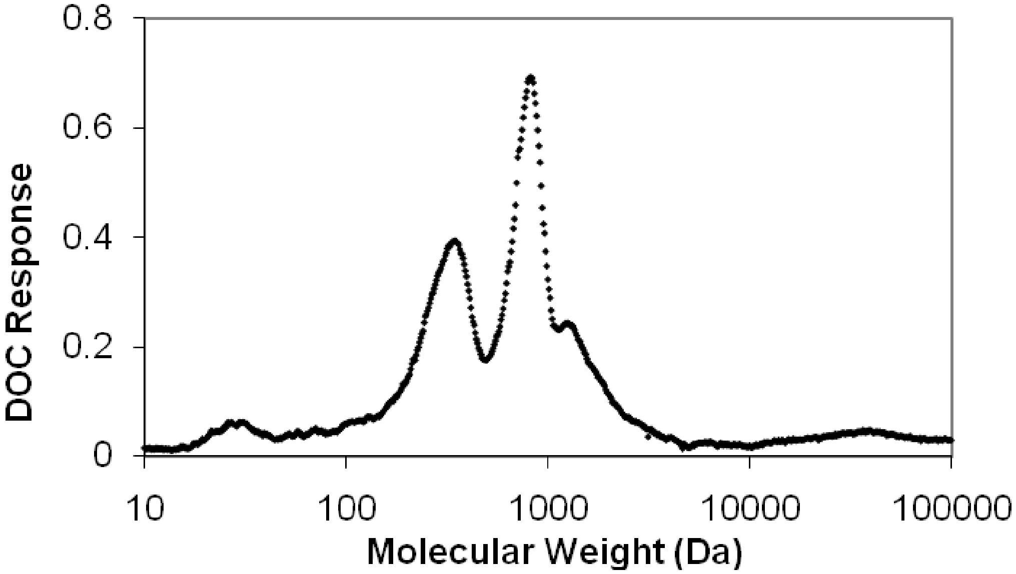

Spring East-West transect (41.9300, 5.2800).

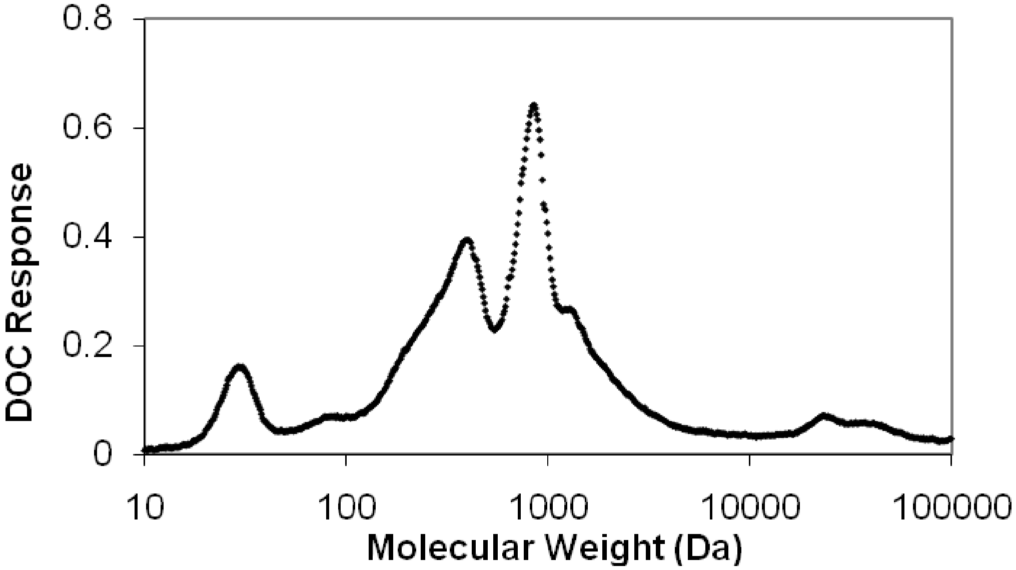

Spring East-West transect (43.5400, 7.2800).

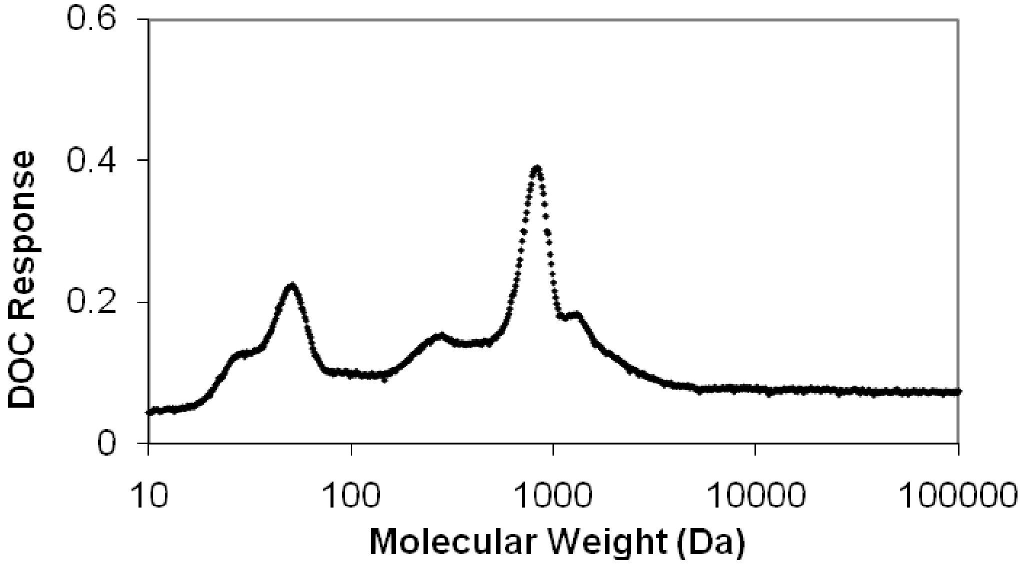

Summer East-West transect (35.8684, 21.2694).

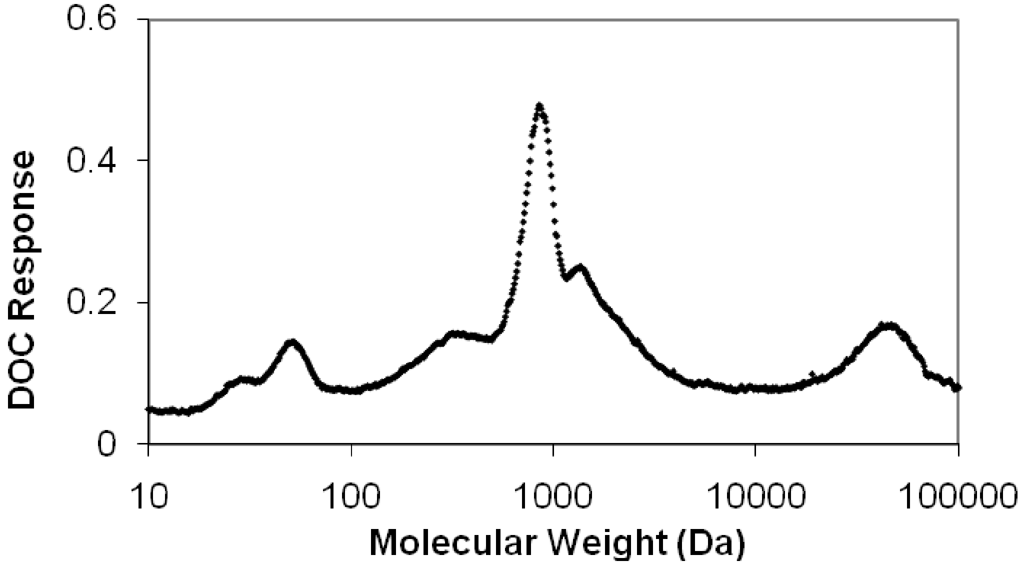

Summer East-West transect (36.1008, 18.5180).

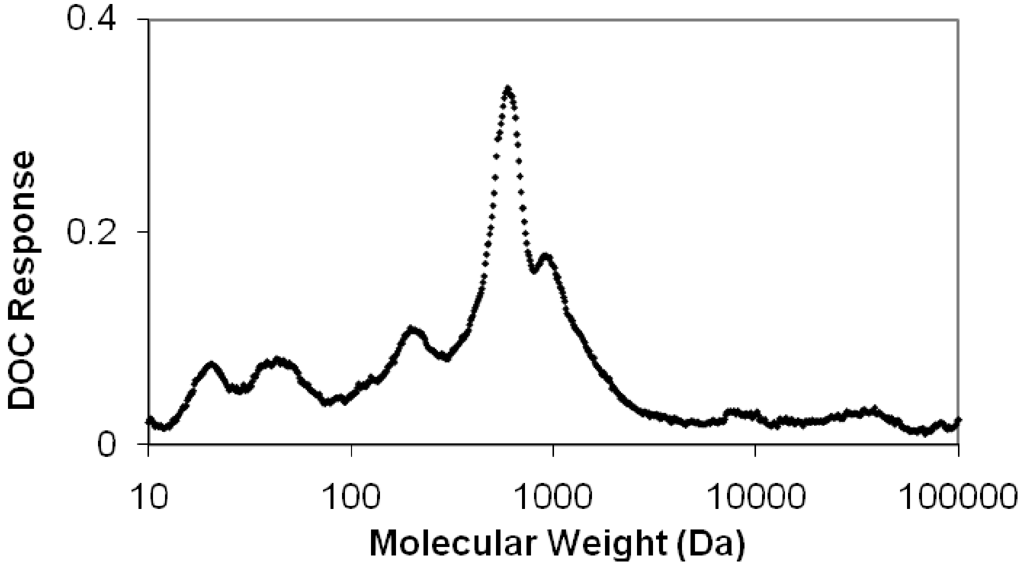

Summer East-West transect (36.2821, 16.4556).

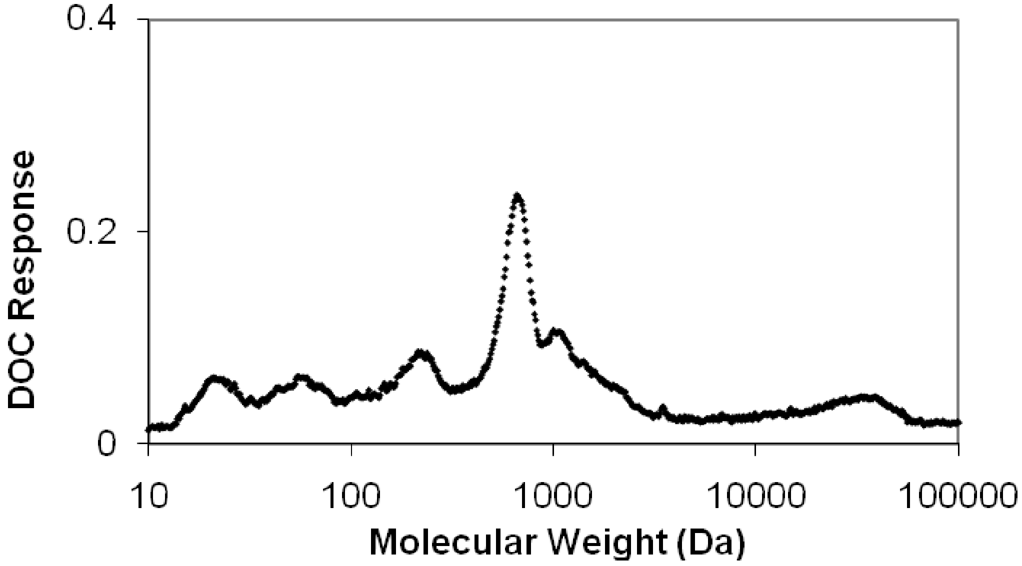

Summer East-West transect (36.8535, 12.9870).

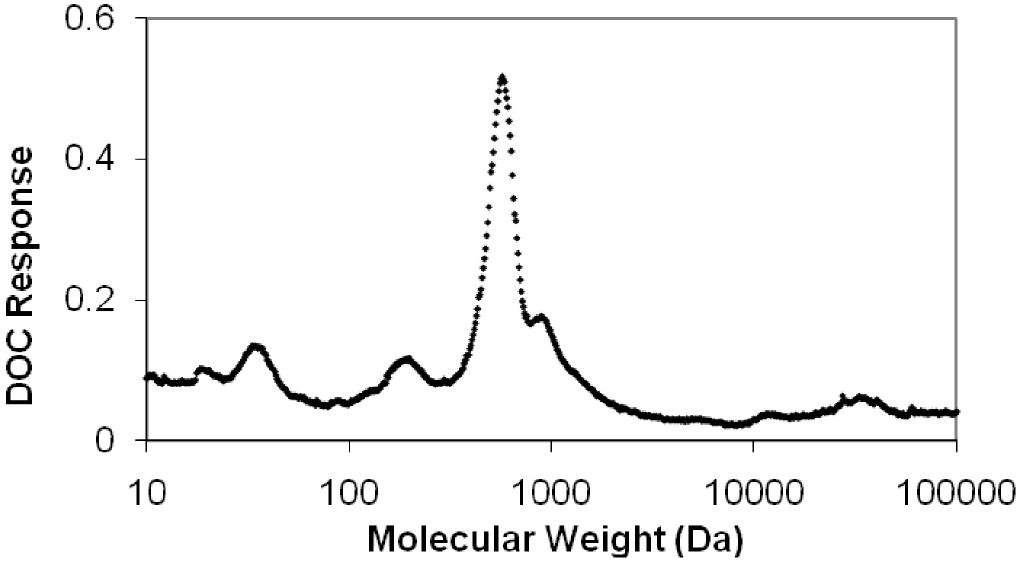

Summer East-West transect (37.7461, 7.8222).

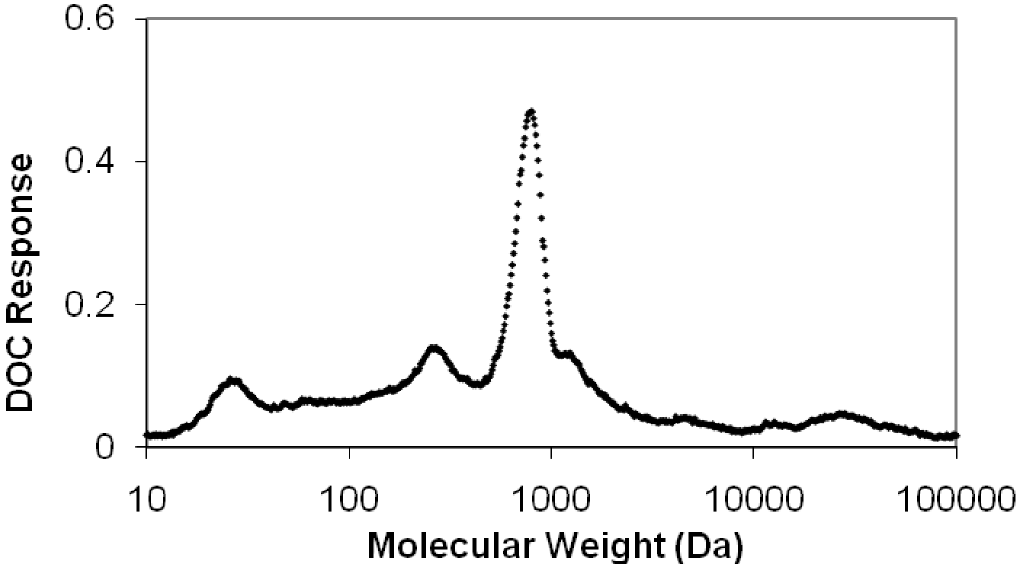

Summer East-West transect (37.1840, 2.1992).

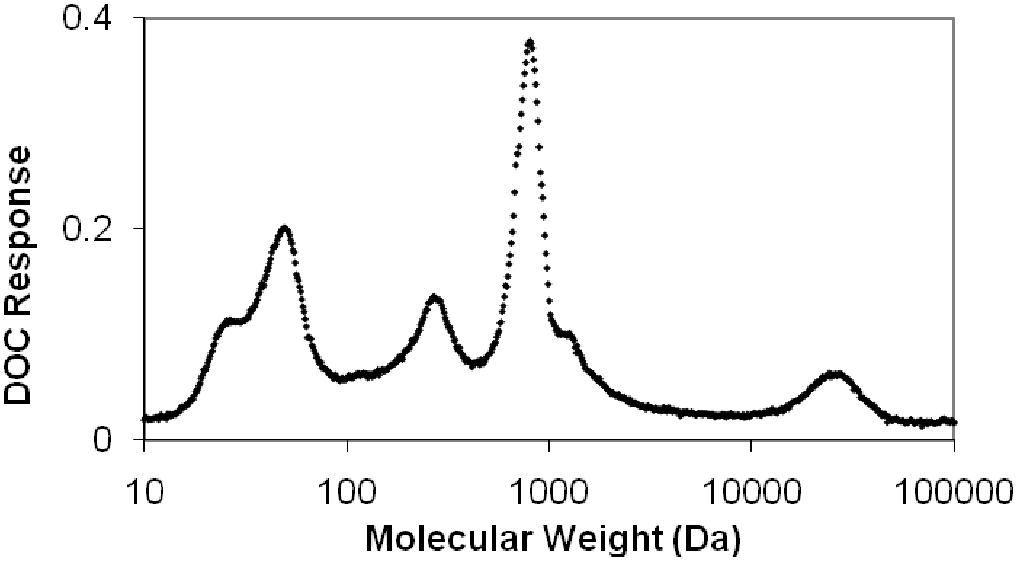

Summer East-West transect (36.3658, -2.5889).

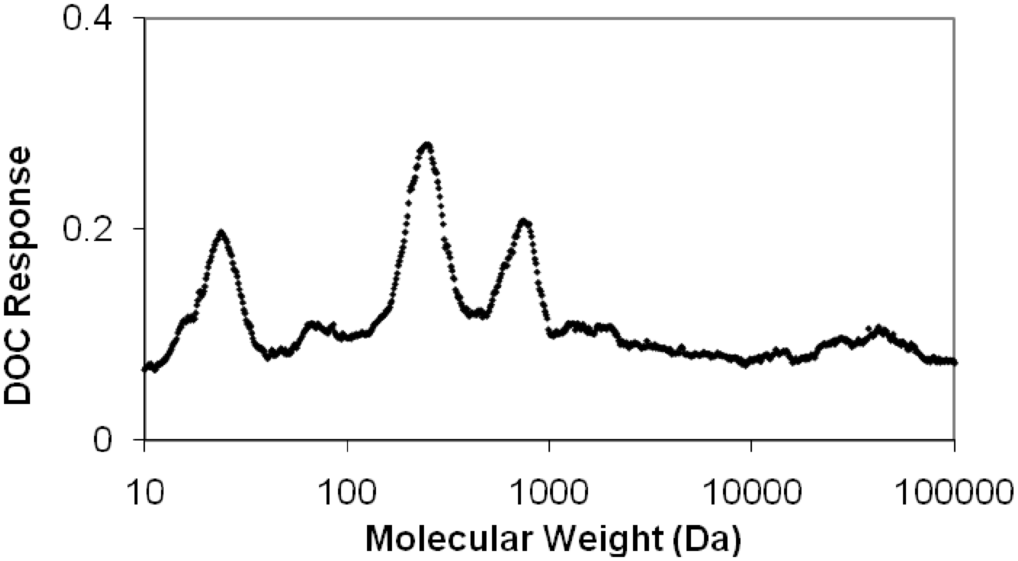

Summer East-West transect (35.9787, -6.9715).

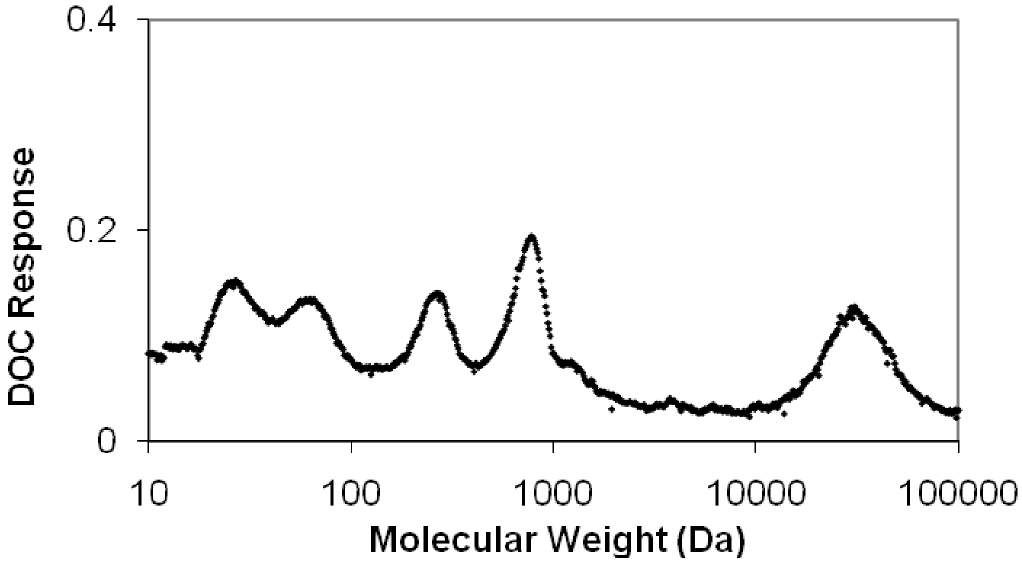

Summer East-West transect (36.0309, -22.0601).

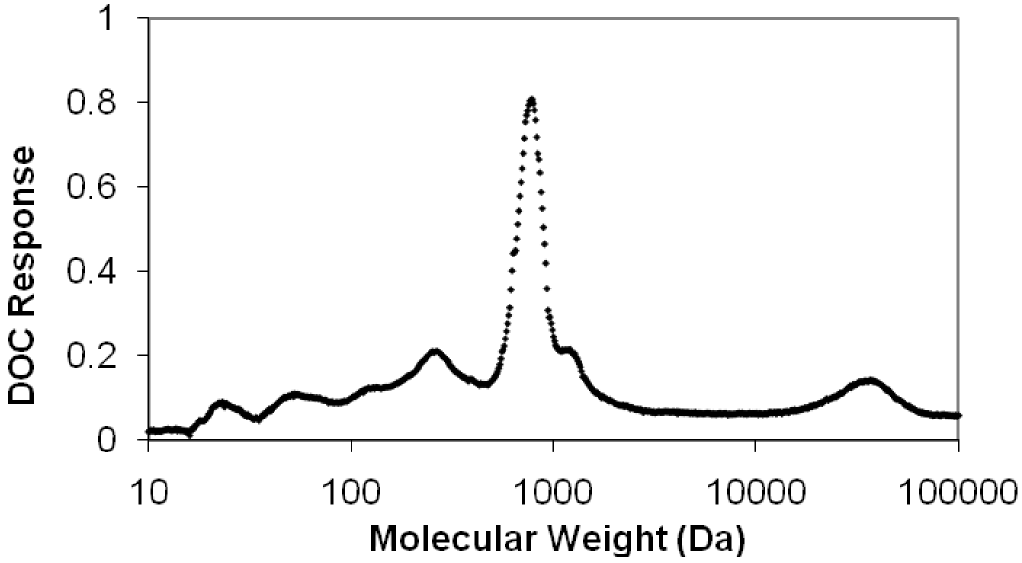

Summer East-West transect (37.1201, -36.3892).

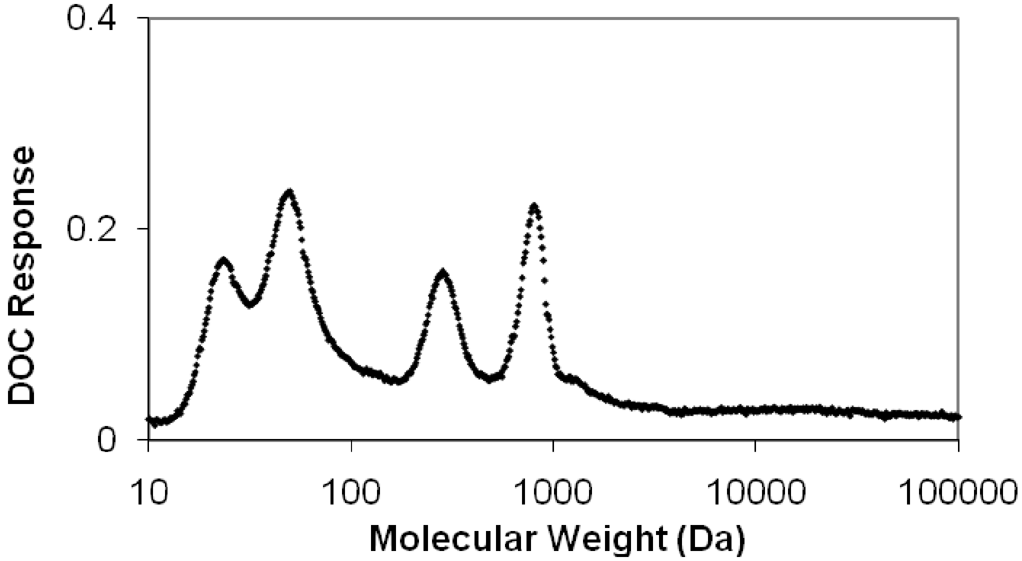

Summer East-West transect (38.5550, -49.6178).

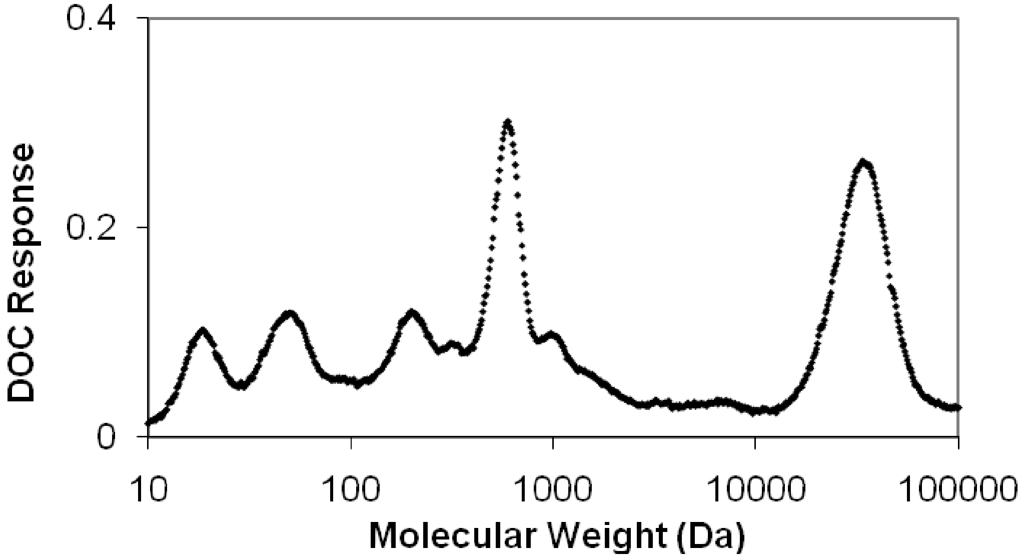

Summer East-West transect (39.6616, -59.6924).

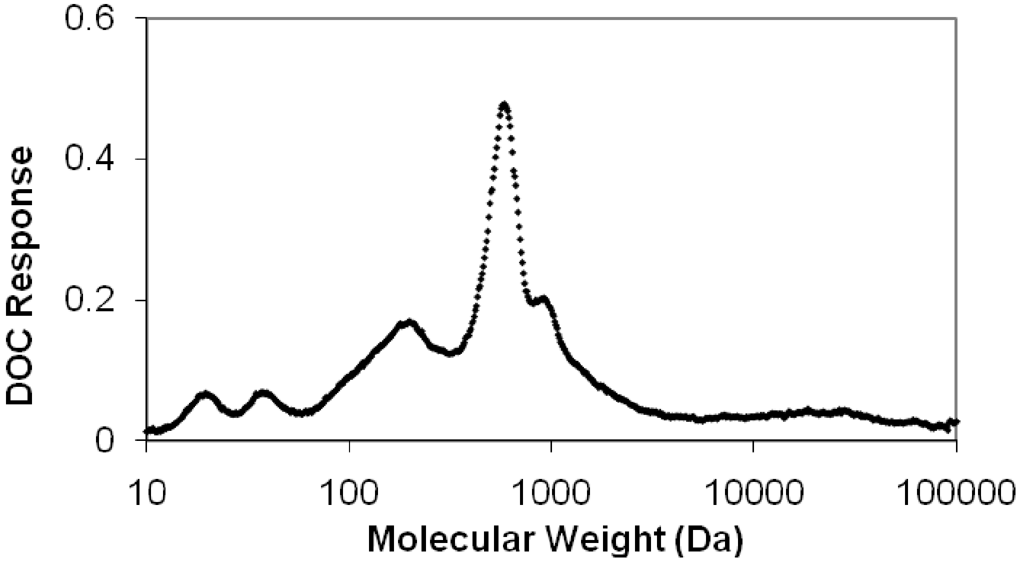

Summer East-West transect (40.4899, -67.6350).